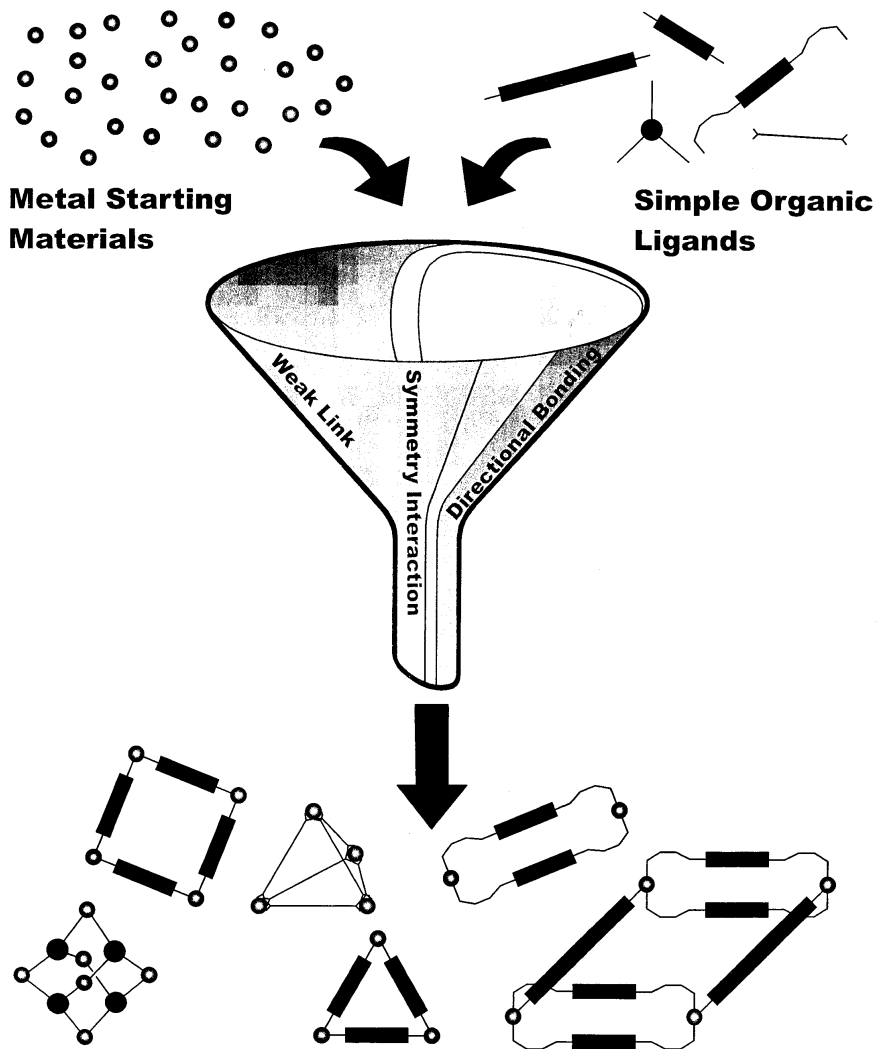
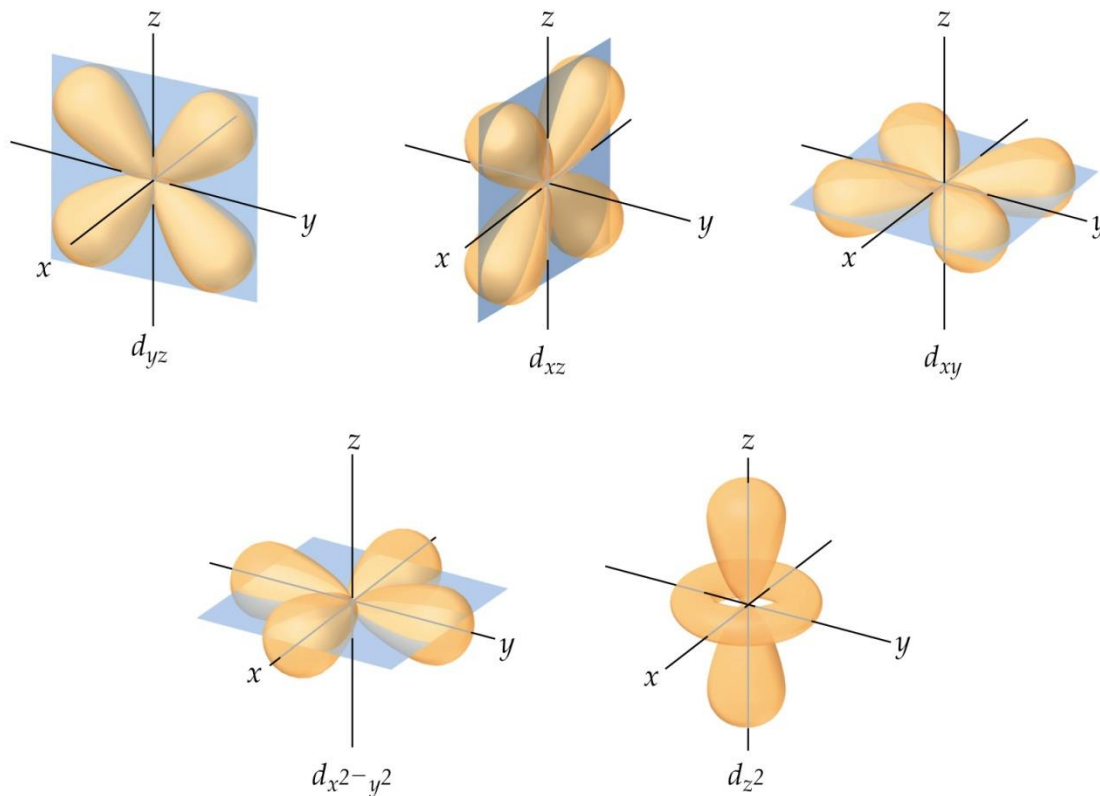


Supramolecular Coordination Chemistry



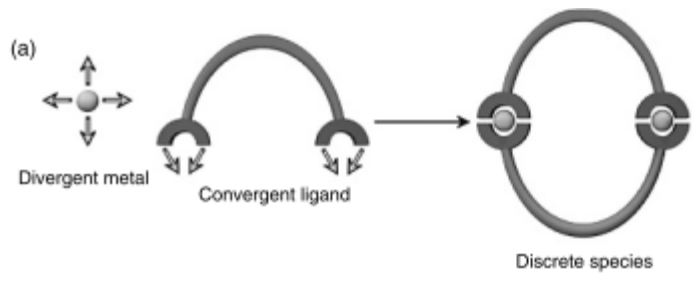
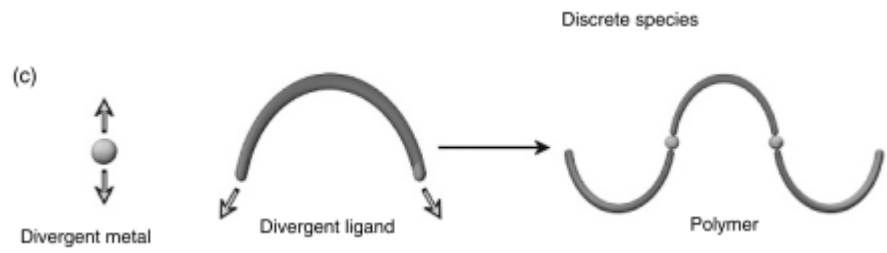
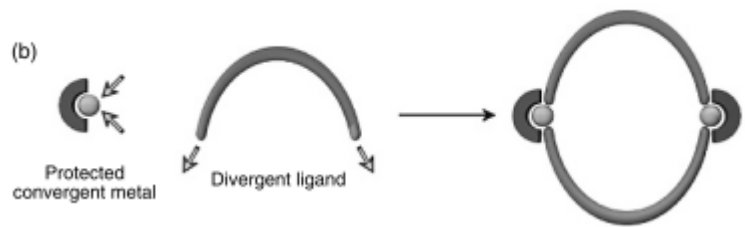
Metal as **connector** :

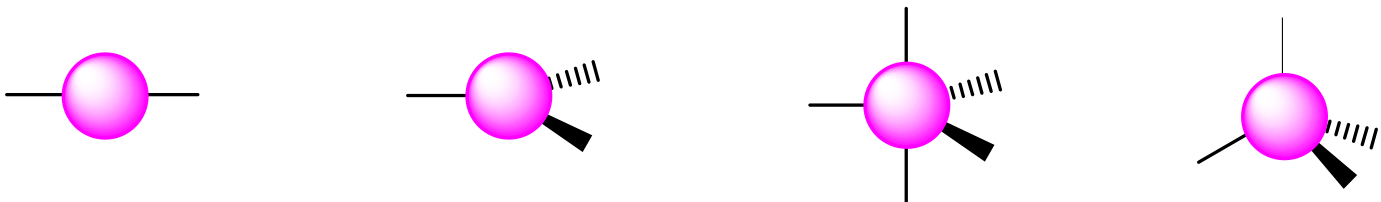
- labile M-L interaction (kinetic)
- stable compound (thermodynamic)
- highly directional with many geometries available



Metal as **functional group** :

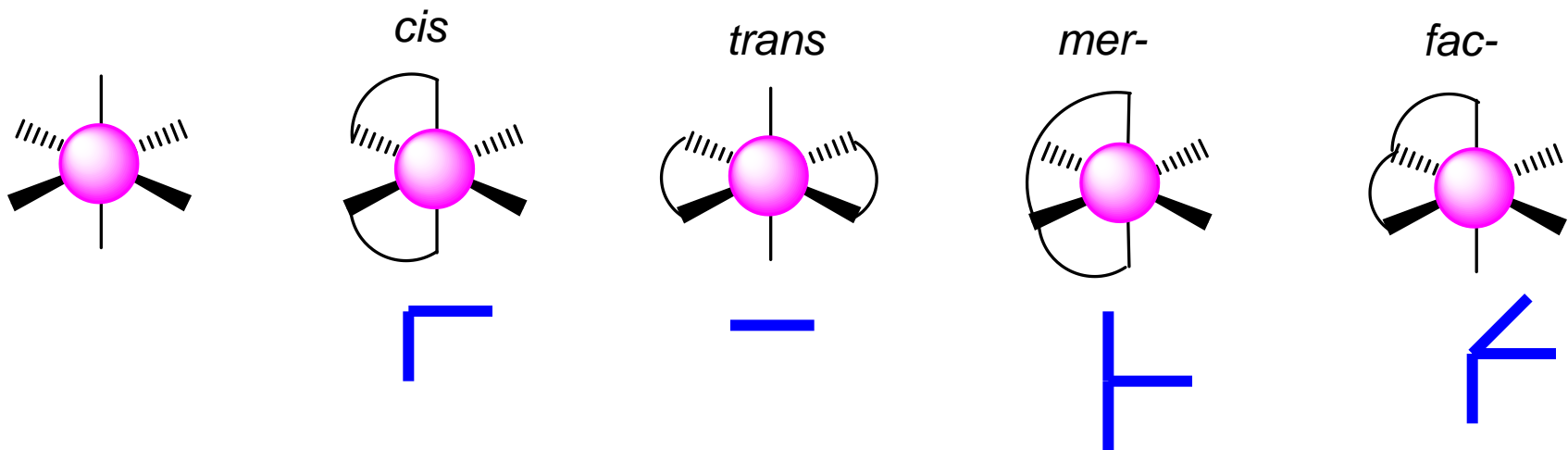
- redox active (electron transfer)
- UV-vis active (color)
- photo active (phosphorescence)
- magnetic properties





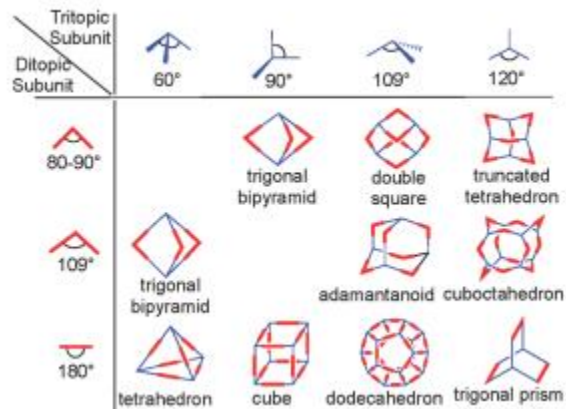
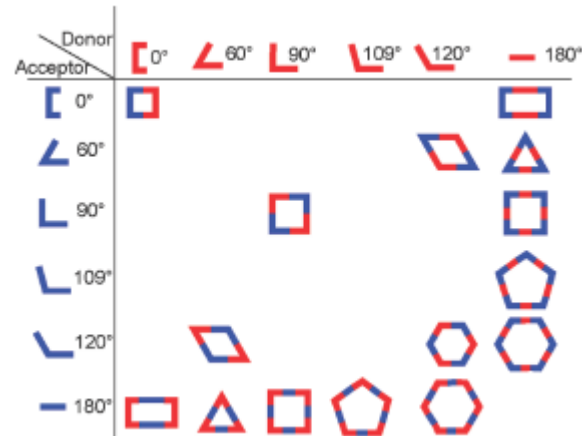
Classical metals used:

Pd(II), Pt(II), Cu(I), Cu(II),
 Re(I), Co(II), Fe(II), Ag(I),
 Zn(II), Ru(II)...



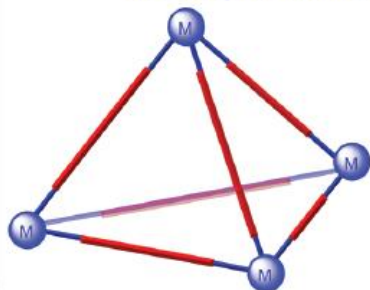
Directonal Bonding Approach

M = bb acido, **L** = bb basico, definiti secondo il numero e geometria relativa dei siti acidi e basici

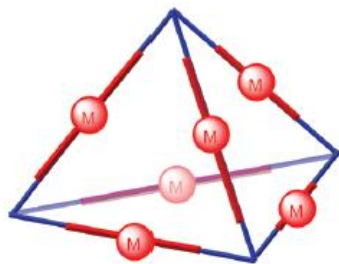


Directional Bonding

60° tritopic subunits + 180° ditopic subunits



M_4L_6

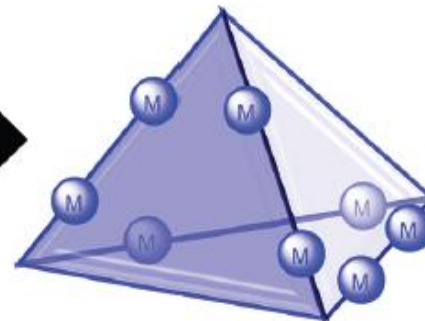


M_6L_4

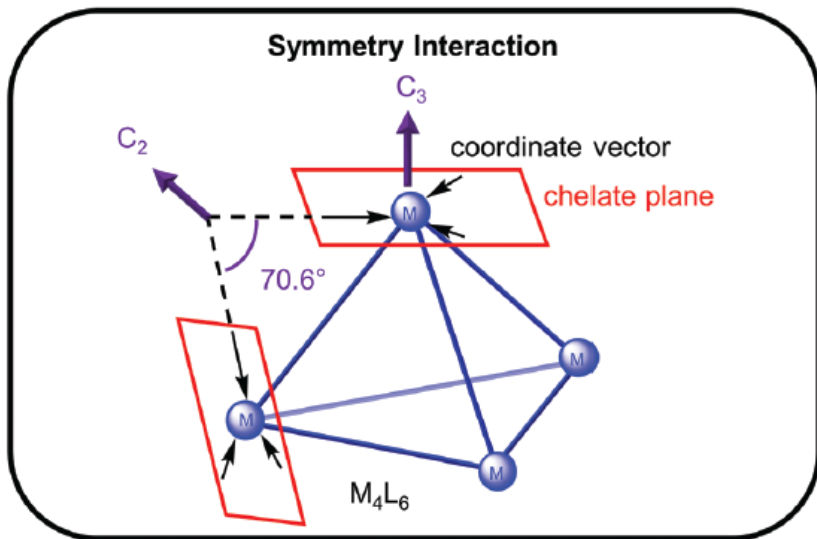
Molecular Panelling



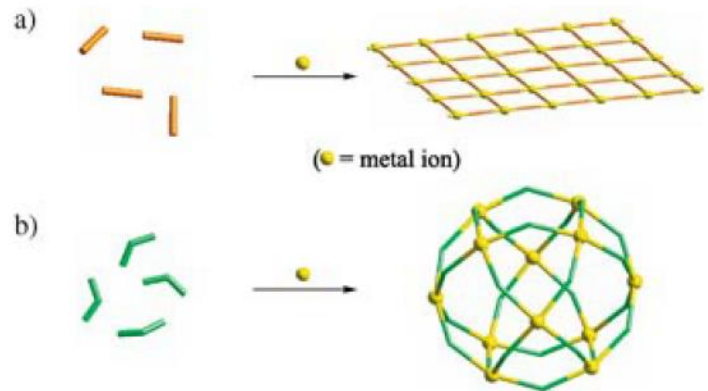
2D panel



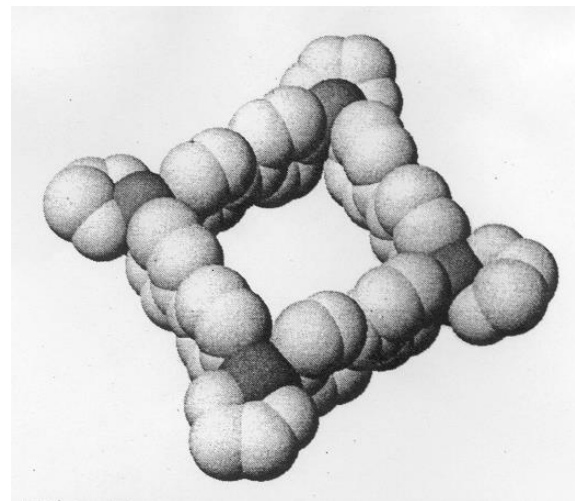
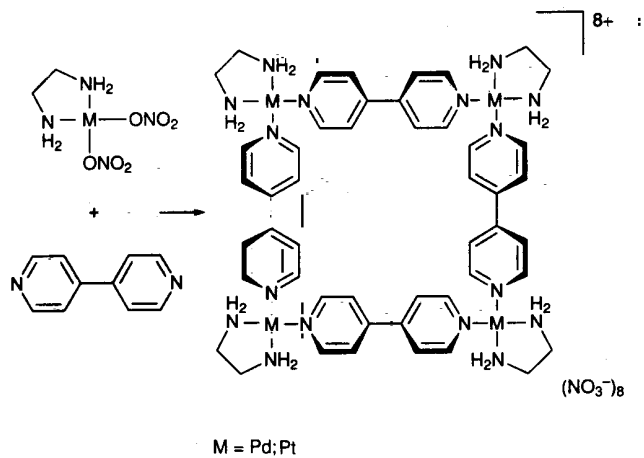
M_8L_4



Banana-shaped ligands



Specie poligonali 2D



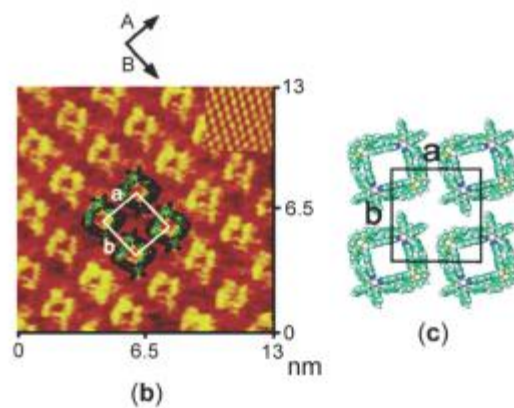
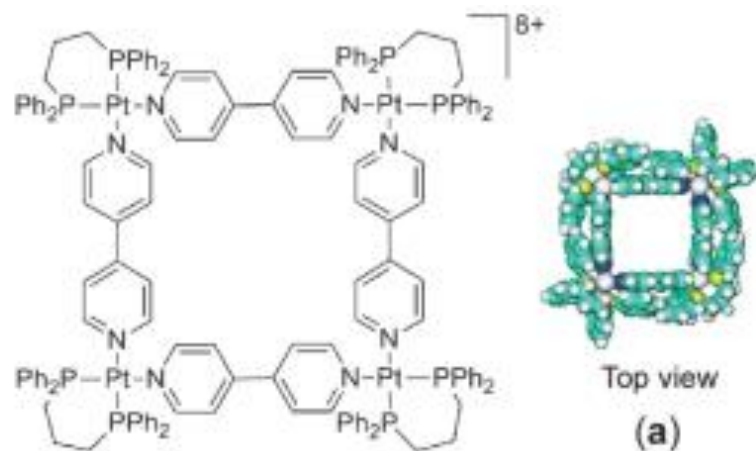
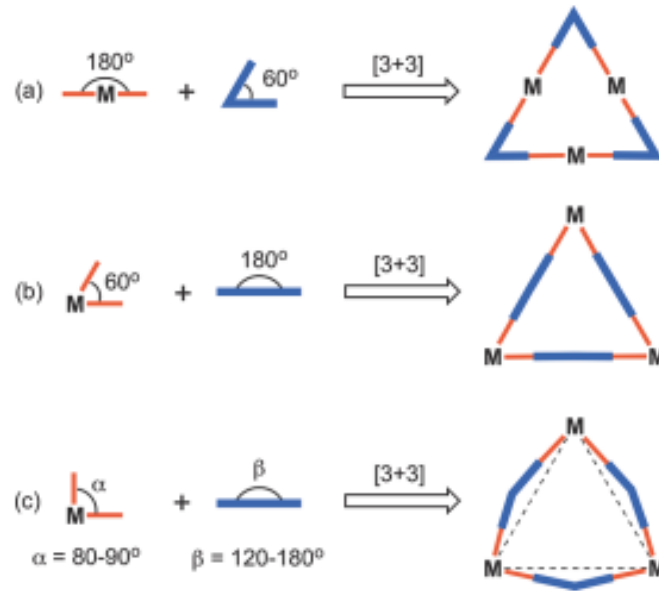
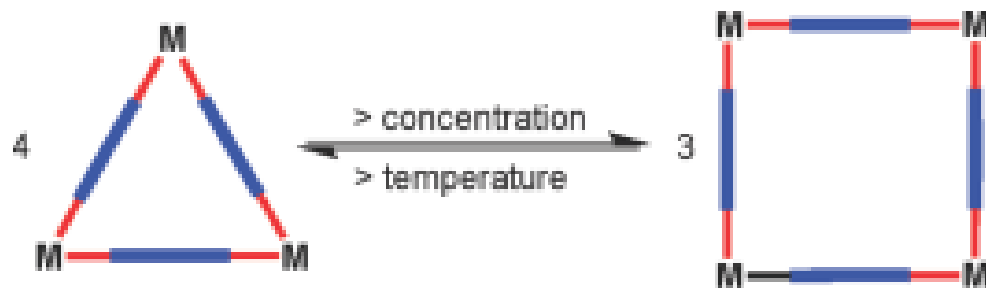


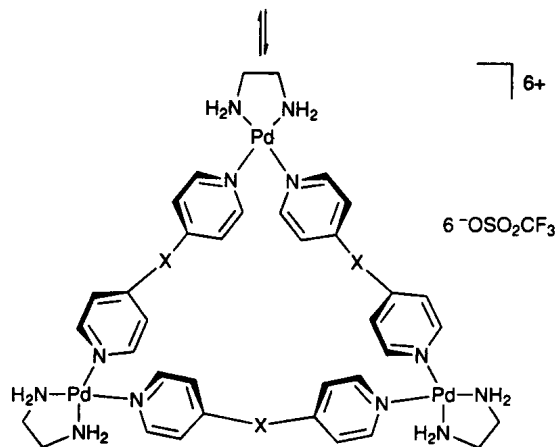
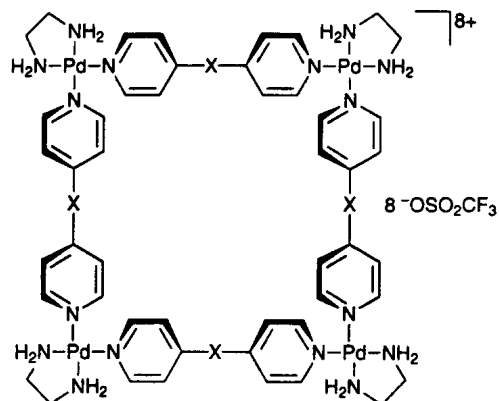
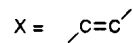
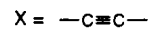
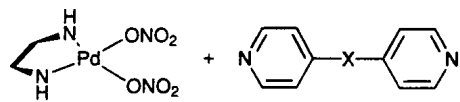
Figure 41. (a) Space-filling model of molecular square $[\text{Pt}(\text{dppp})(4,4'\text{-bipyridine})]_4(\text{PF}_6)_8$, (b) high-resolution STM images of the adlayer of square on Au(111), and (c) structural model of the adlayer.

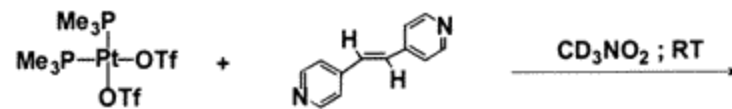
Triangoli Molecolari





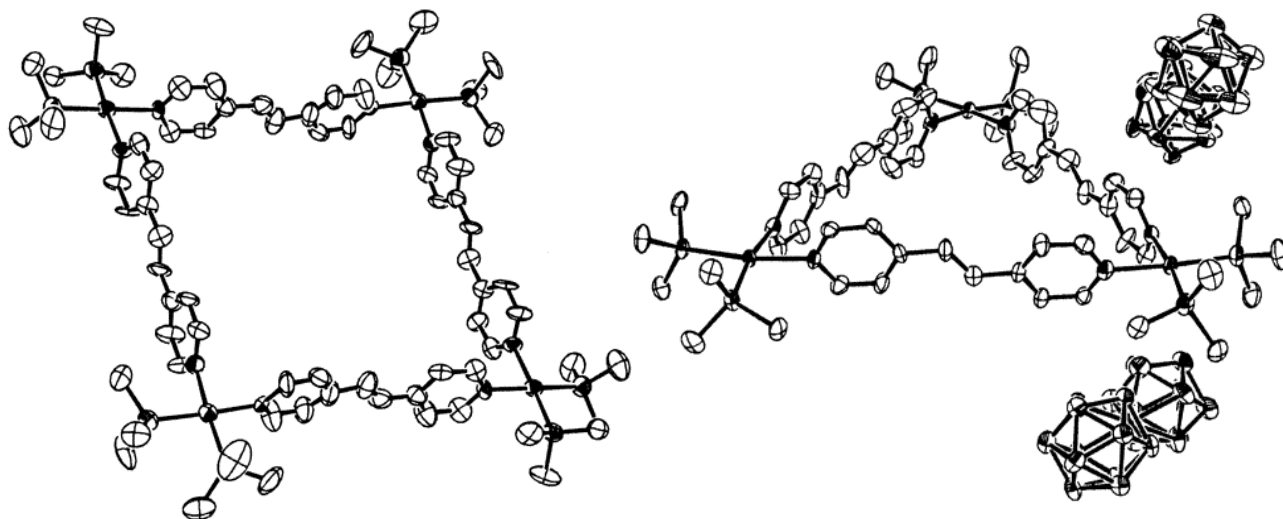
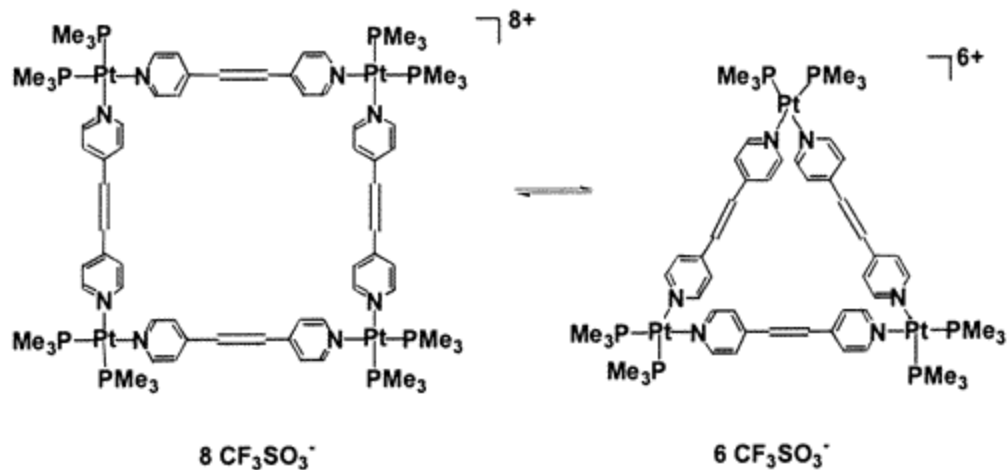
Solvent
Concentration
Temperature

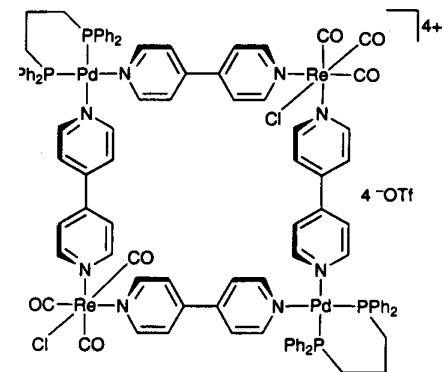
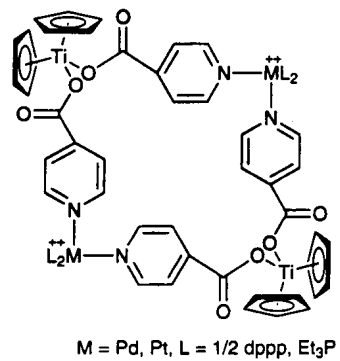
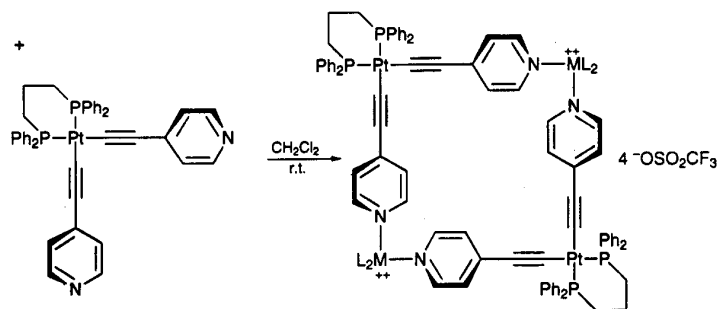
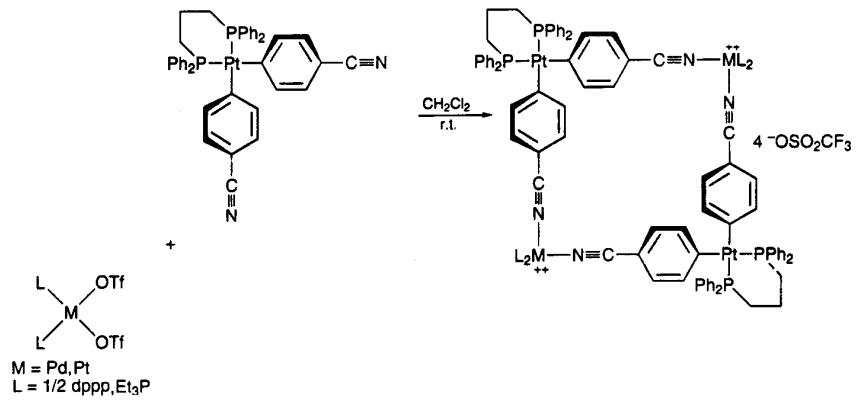


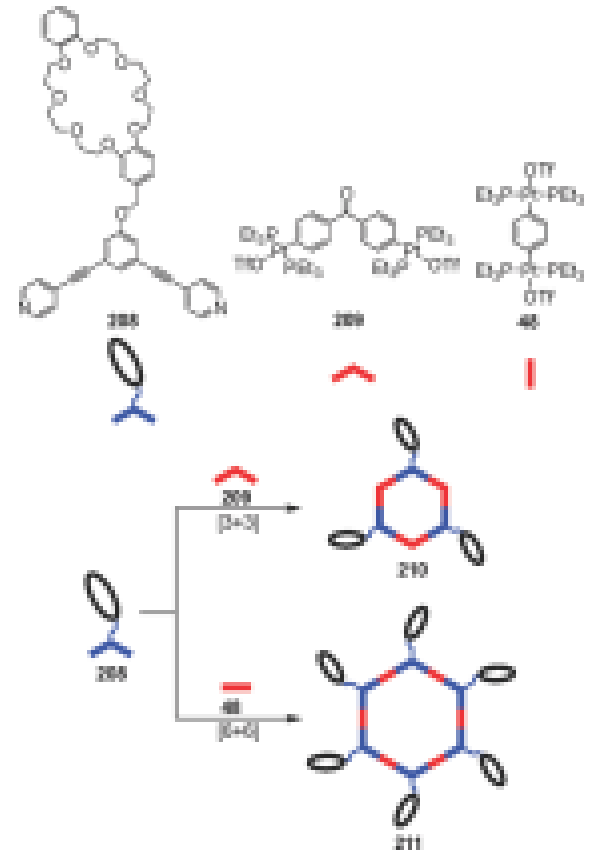
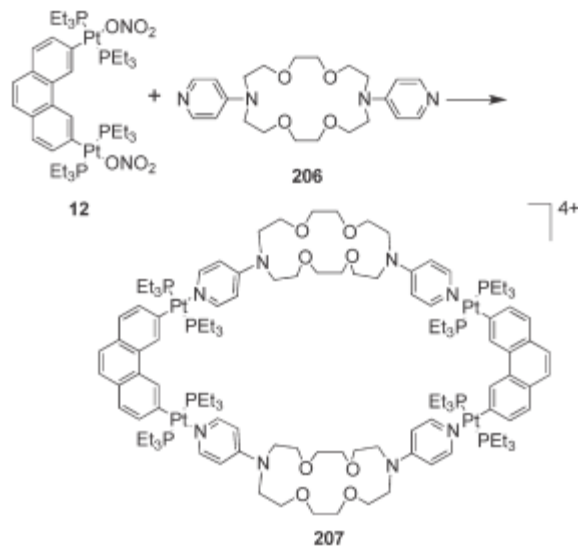
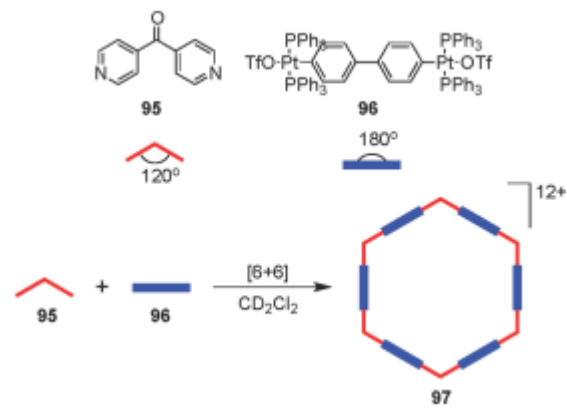


1

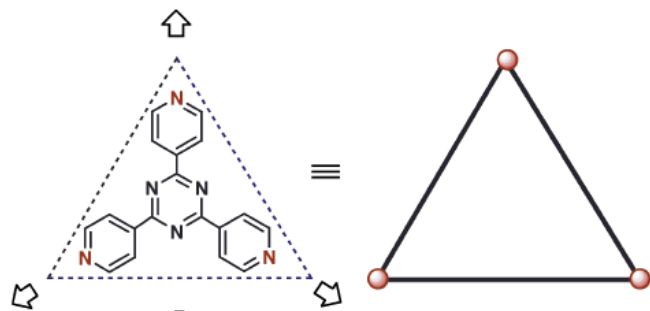
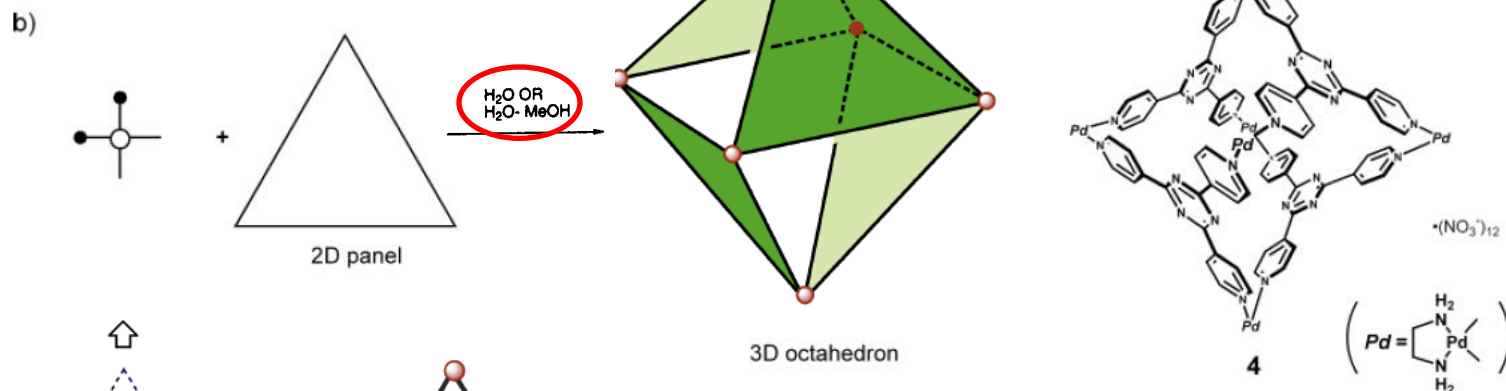
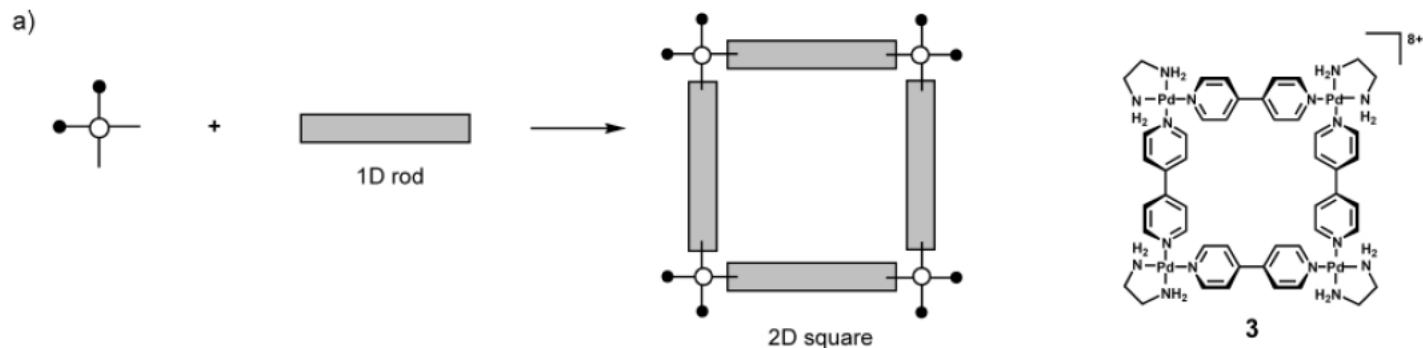
2



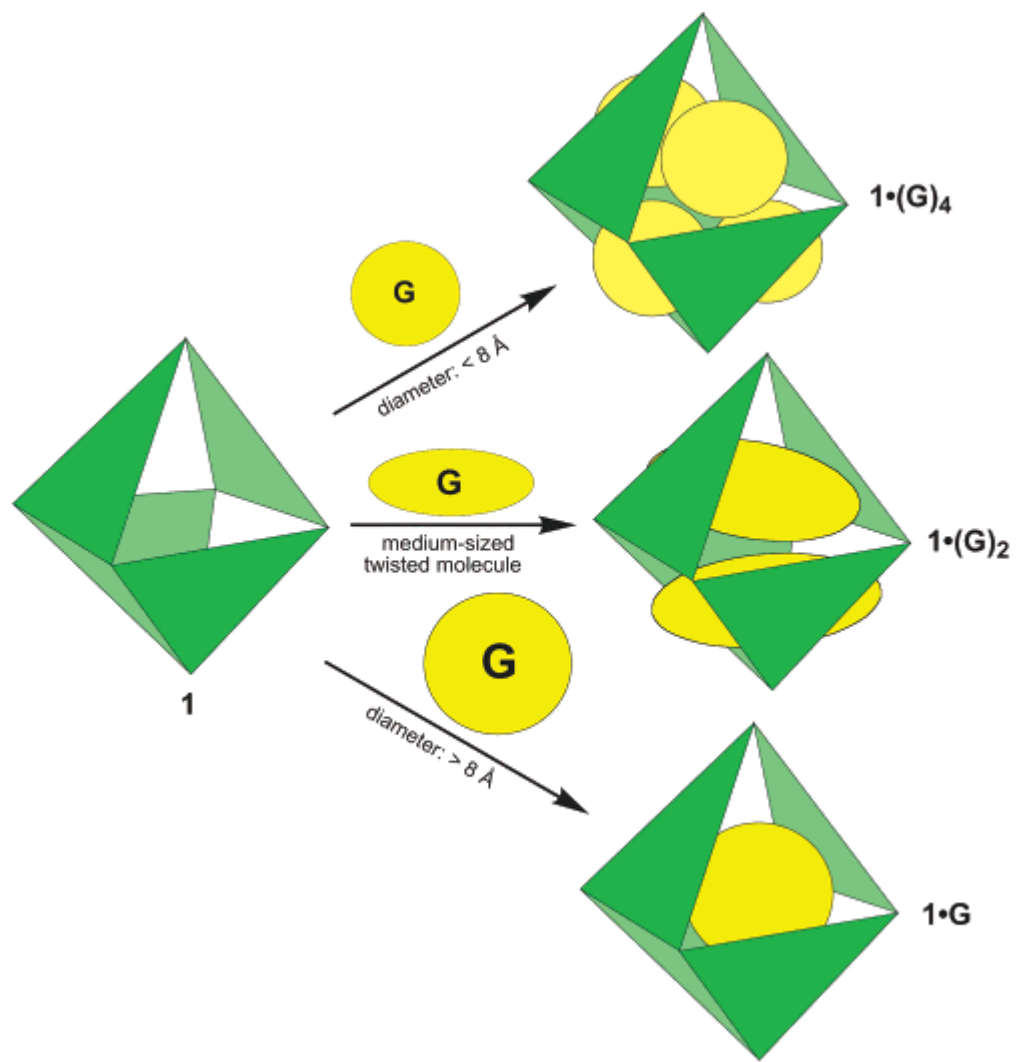
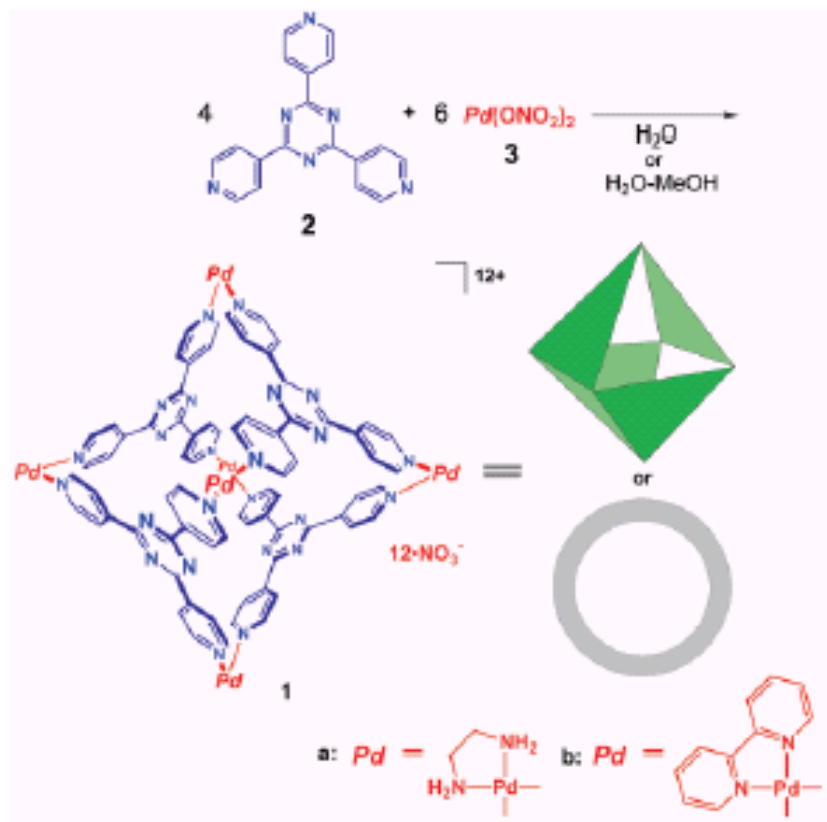




Makoto Fujita,* Kazuhiko Umemoto, Michito Yoshizawa, Norifumi Fujita, Takahiro Kusakawa and Kumar Biradha



M₆L₄
d ca. 11 Å
Portali 8 Å



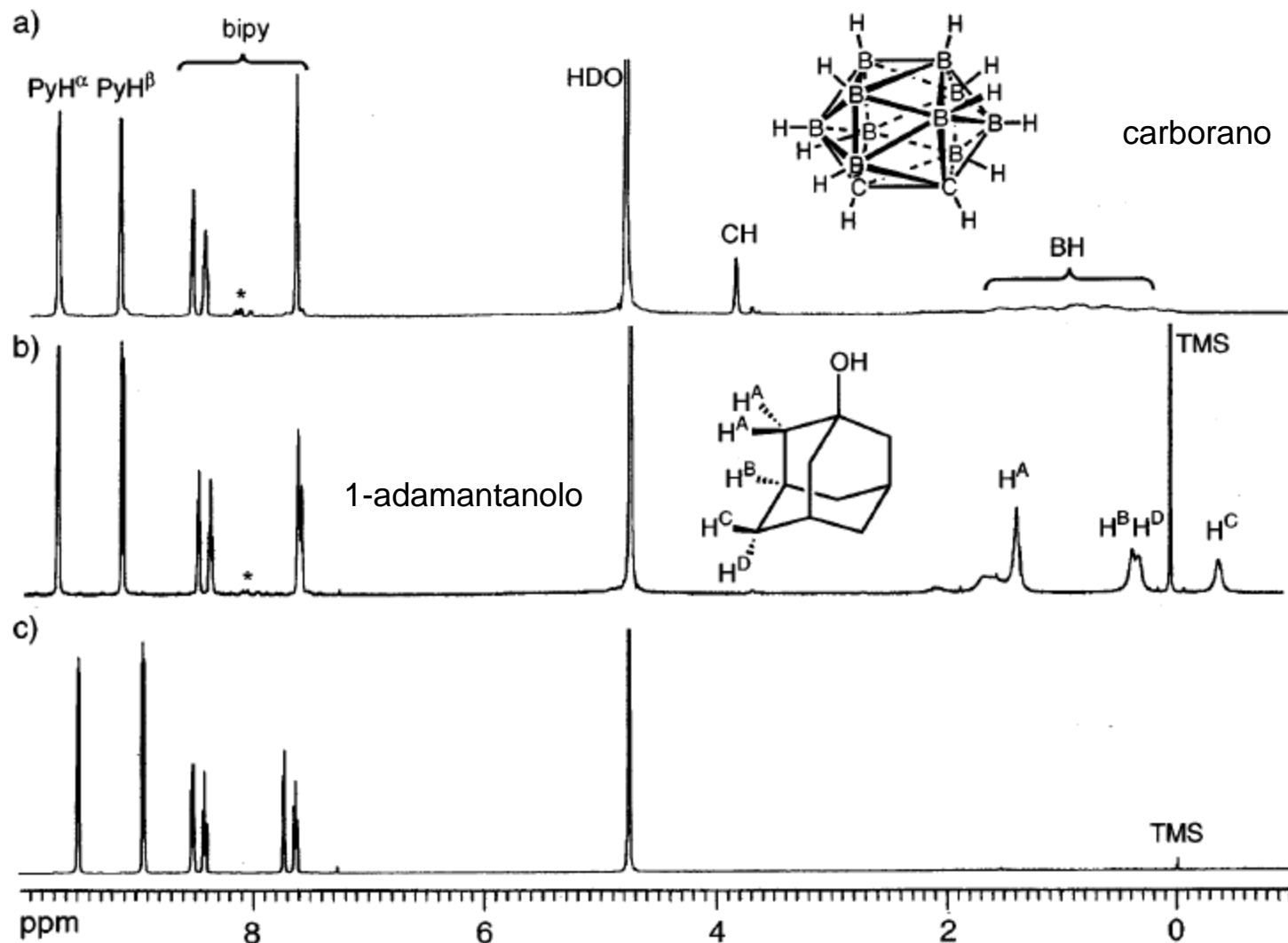
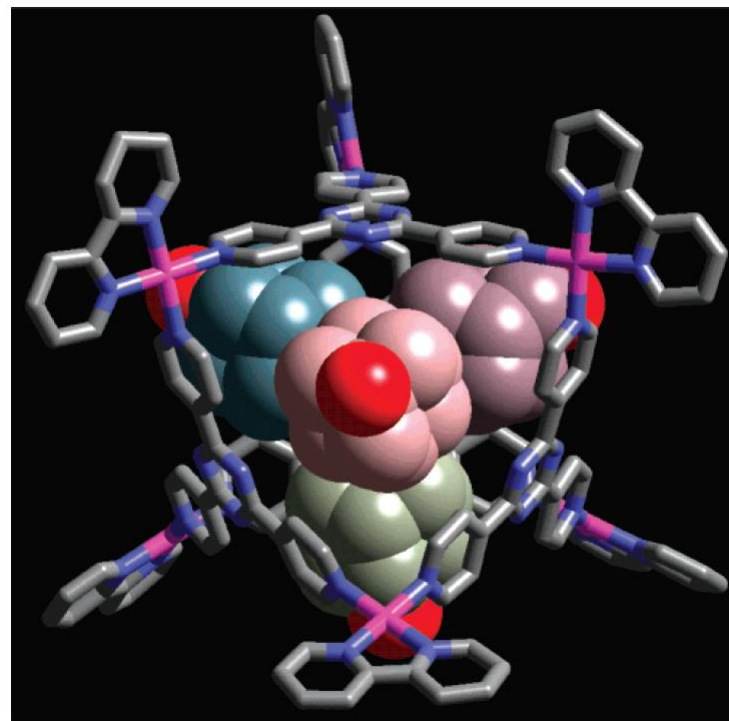
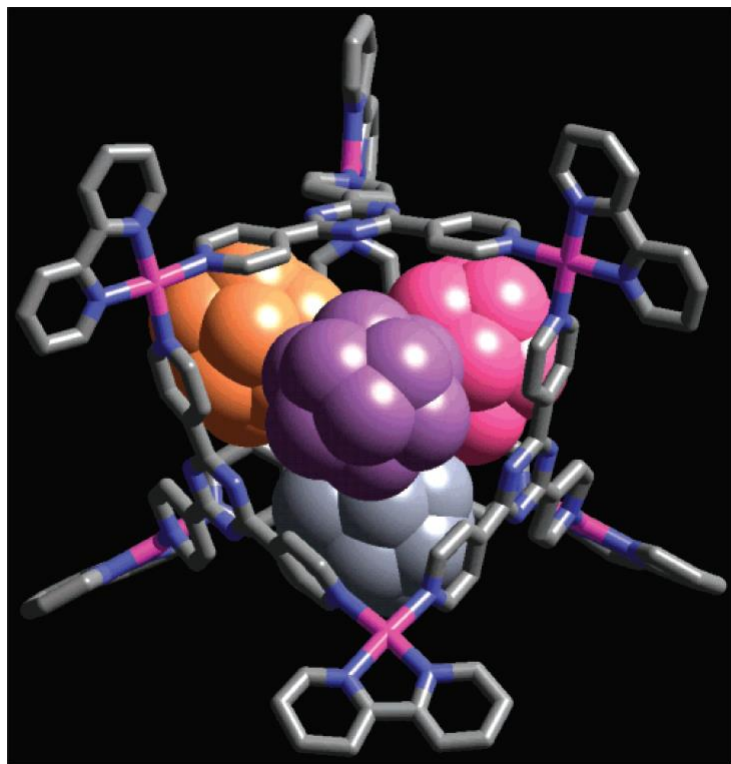
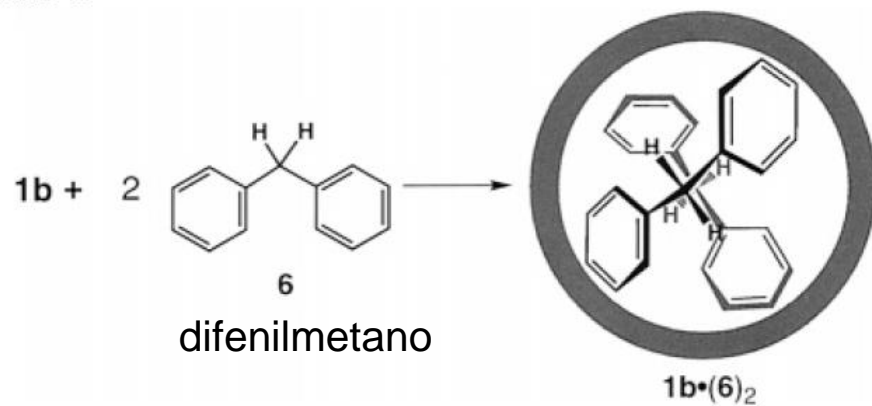


Figure 1. ^1H NMR observations of the enclathration of guest molecules in 1b . (a) $1\text{b}\cdot(4)_4$. (b) $1\text{b}\cdot(5)_4$. (c) Empty 1b (*: impurities).

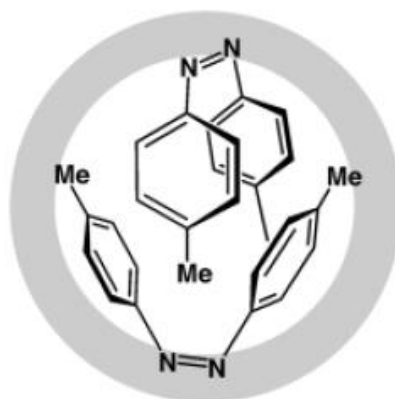


Scheme 2

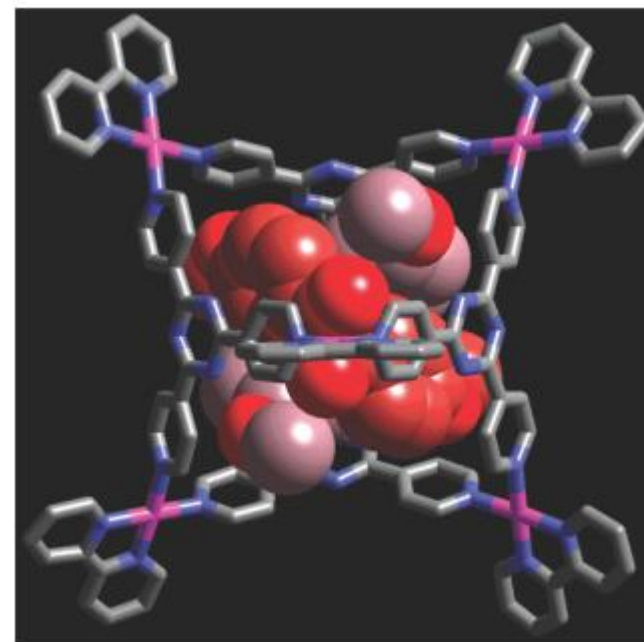
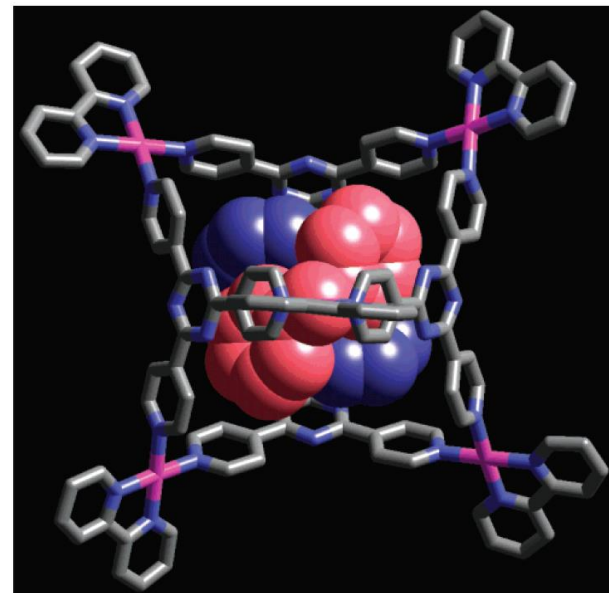
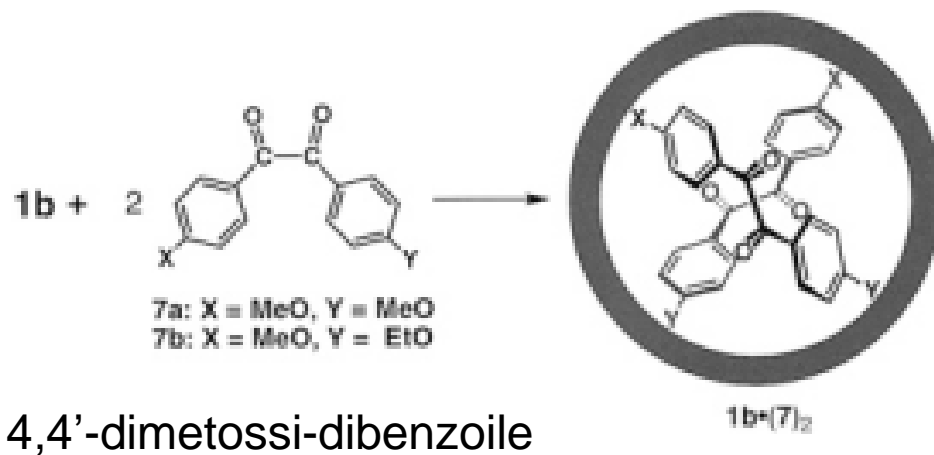


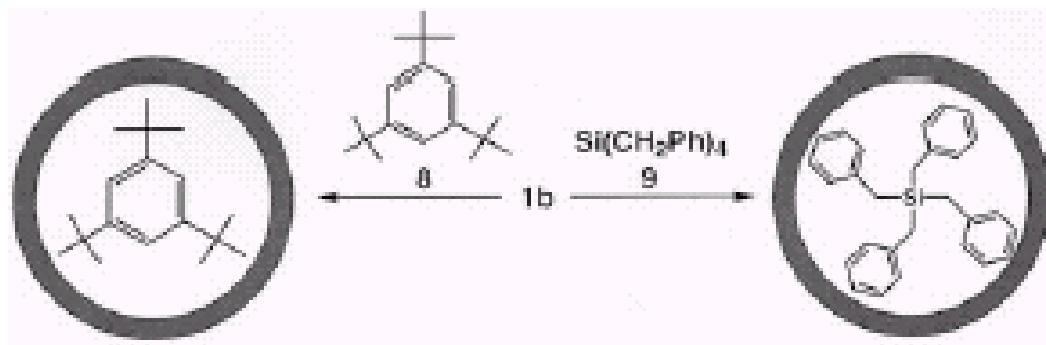
cis-azobenzene

cis-stilbene



Scheme 3





tri-*tert*-butylbenzene

tetrabenzilsilano

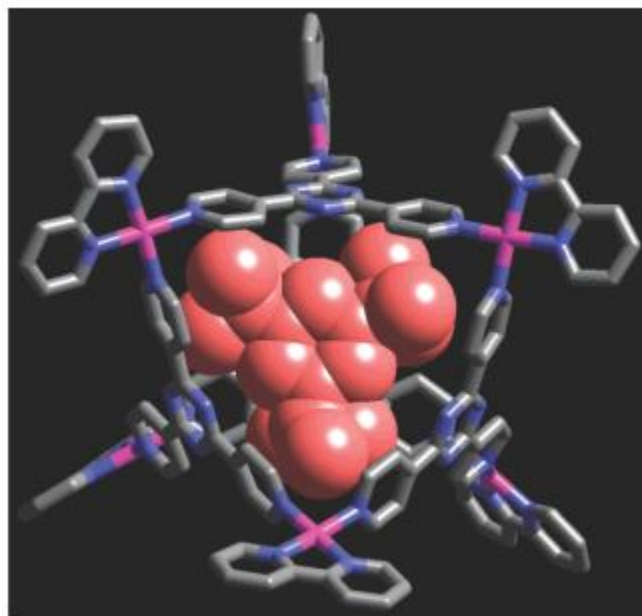
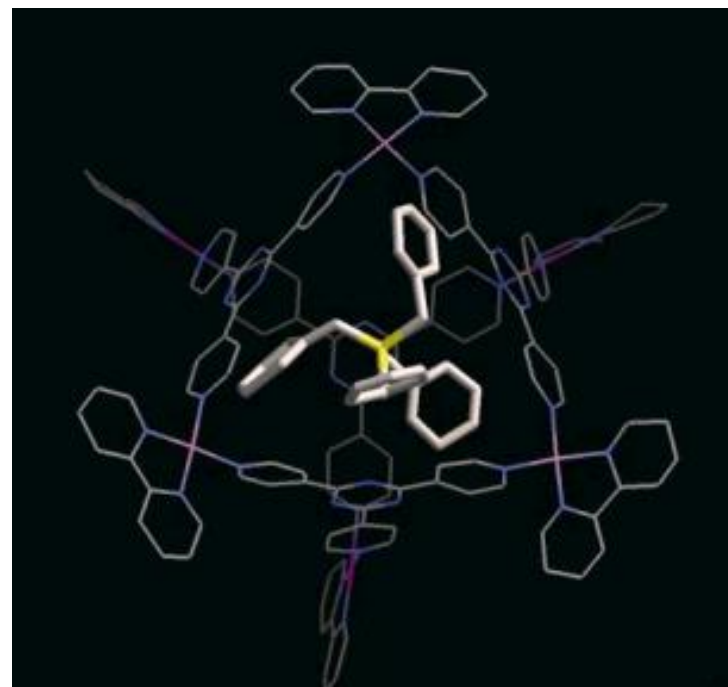
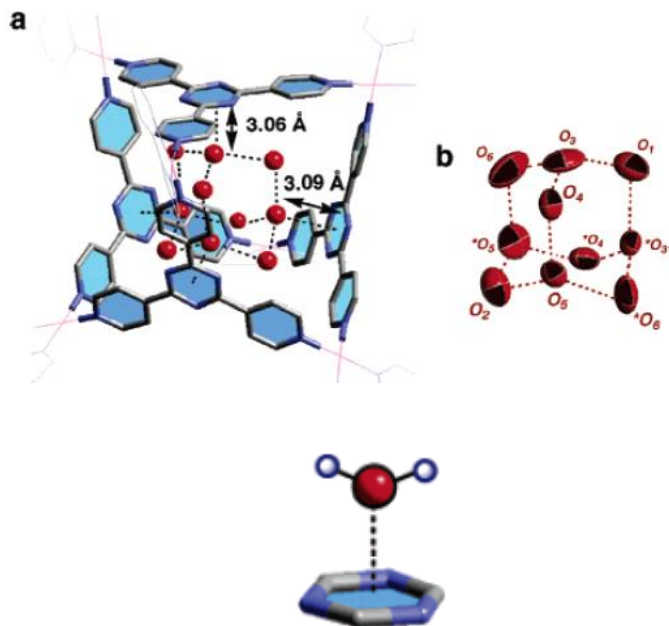
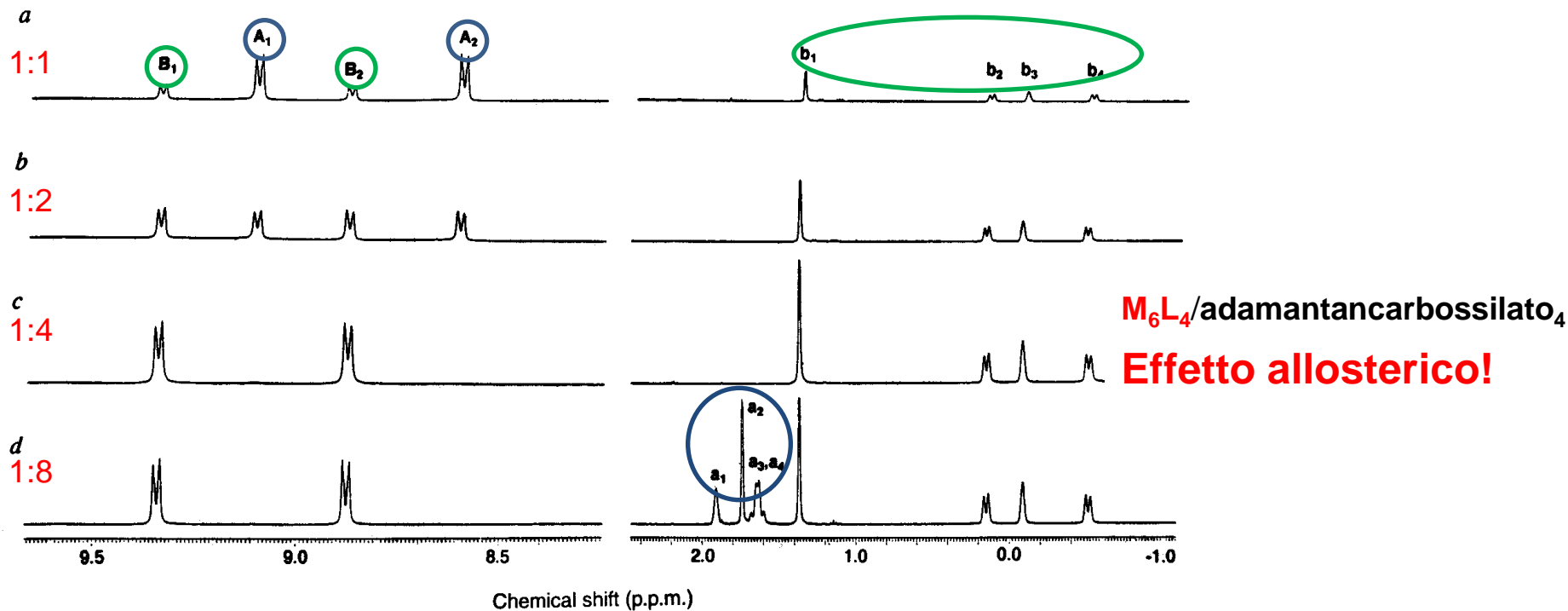


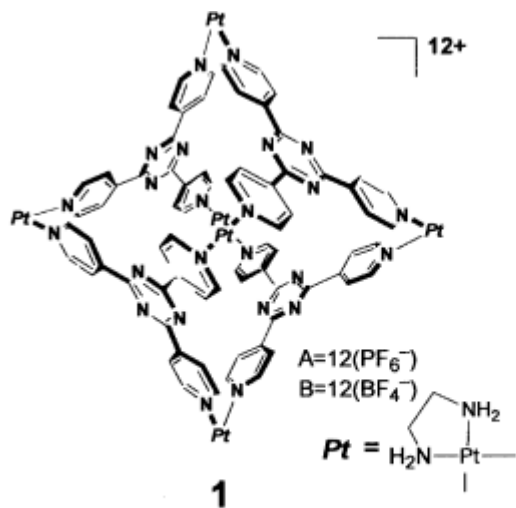
Figure 8. Crystal structure of 1b·8.





I_c-type ice.^{1,2} The X-ray structural analysis, coupled with neutron diffraction study, reveals that the molecular ice is not simply formed by filling the void space but is a result of specific H₂O:⋯π interaction within the cage. Whereas there are numerous examples cluster of hypothetical reversed hydrate complexes. Surprisingly, the molecular ice does not “melt” even at room temperature; the adamantanoid framework of 10 water molecules can be located roughly even in a room-temperature diffraction study.

The presence of highly ordered water clusters inside the binding pockets of proteins has been predicted¹⁵ and considered to be crucial in entropy-driven substrate binding.¹⁶ We suggest that the molecular recognition by cage **1** is entropy-driven, in which the binding of guests is compensated by the “melting” of the molecular ice into free water molecules. The endohedral water cluster therefore plays



a: (C₈₄H₉₆N₃₆Pt₆)¹²⁺•12(PF₆⁻)
FW. 4519.98

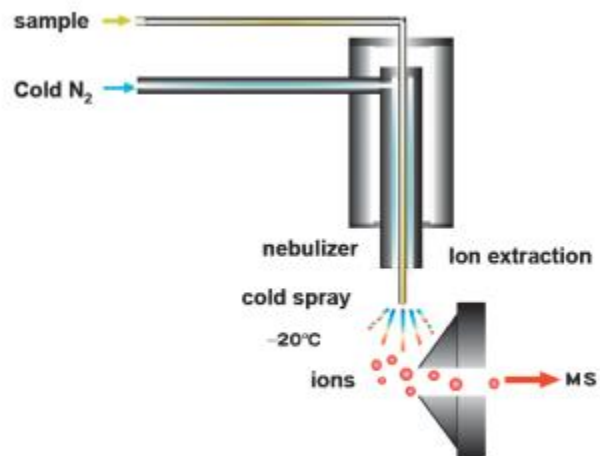


Fig. 1. Schematic illustration of the cold spray.

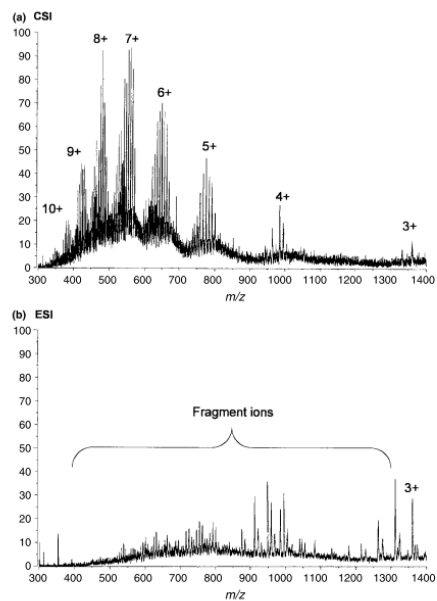
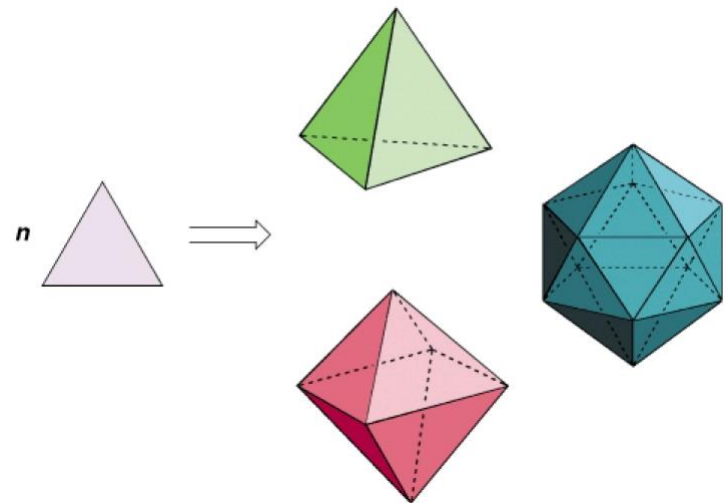
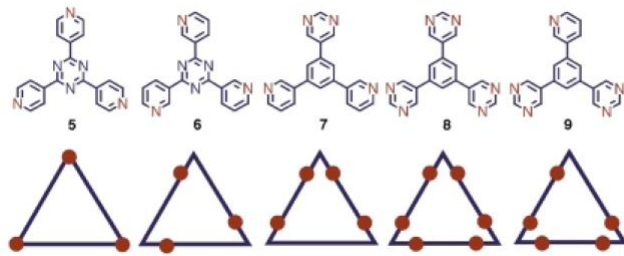
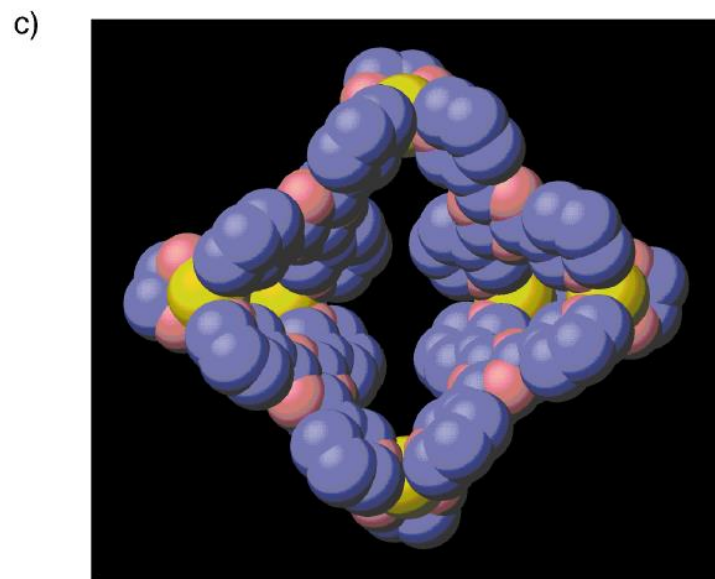
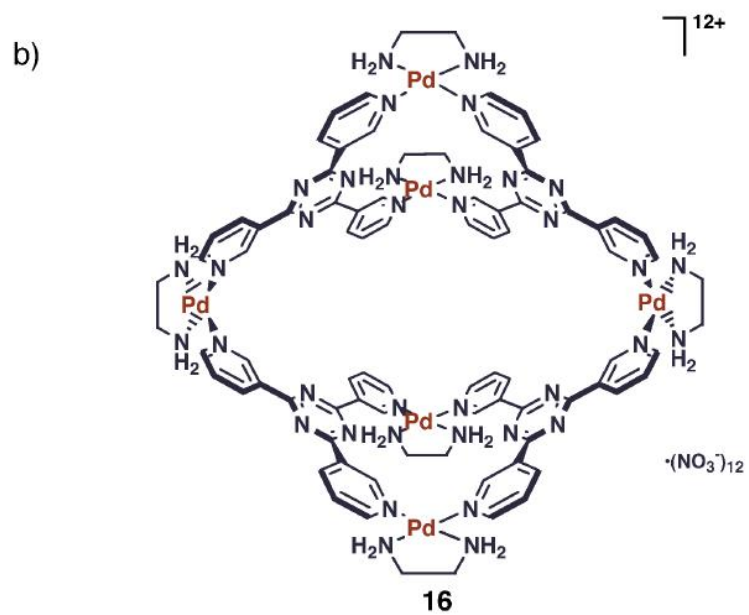
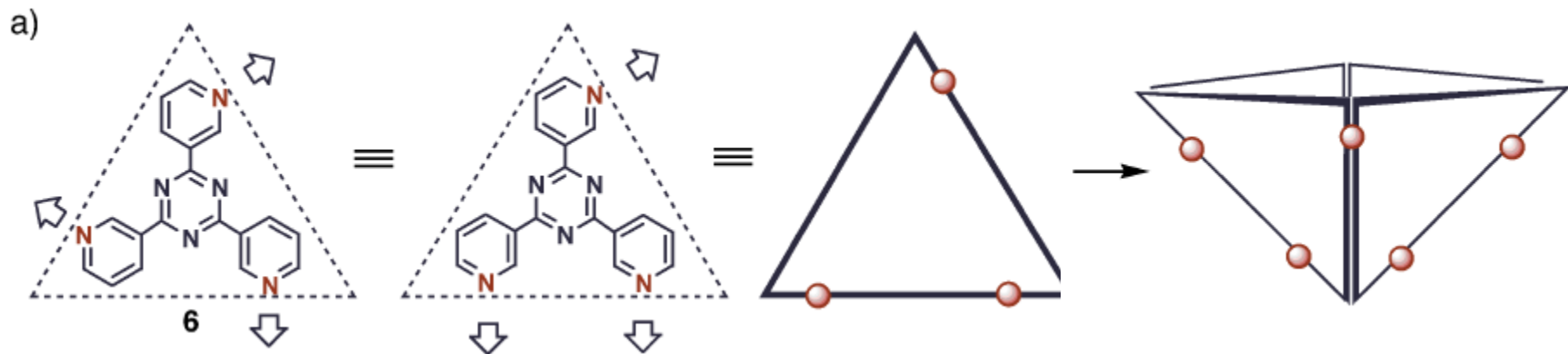


Figure 3. Comparison of (a) CSI and (b) ESI mass spectra of **1a**. Reprinted from Ref. 2 with permission from Elsevier.

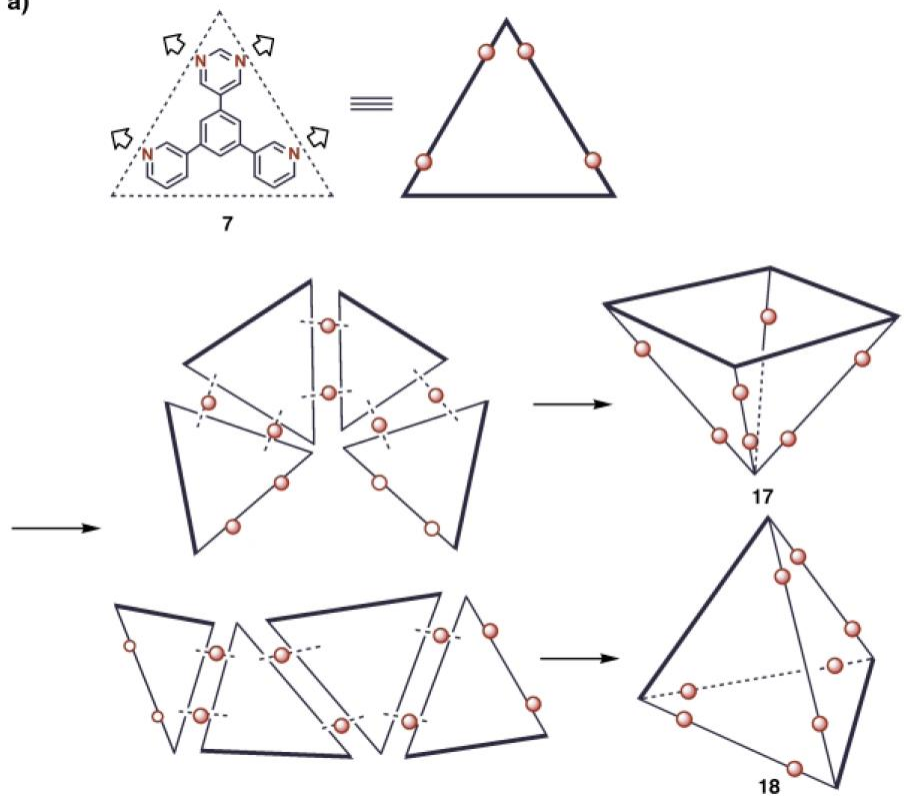
Molecular Paneling

a)



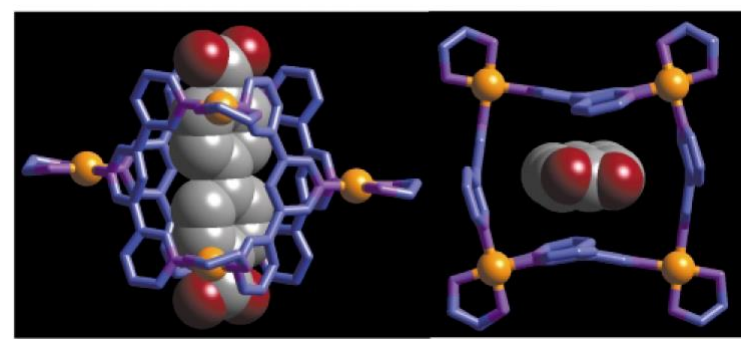
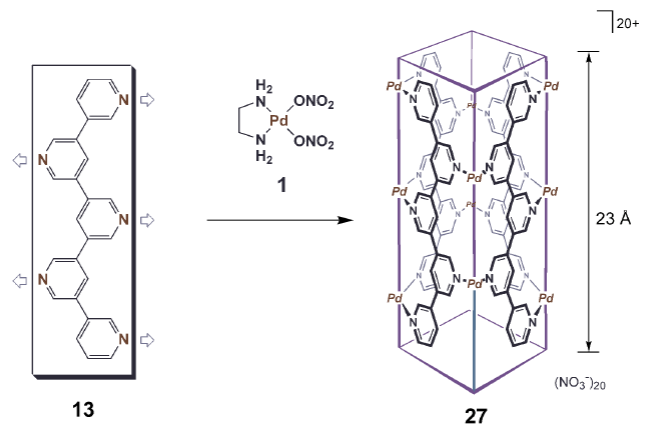


a)

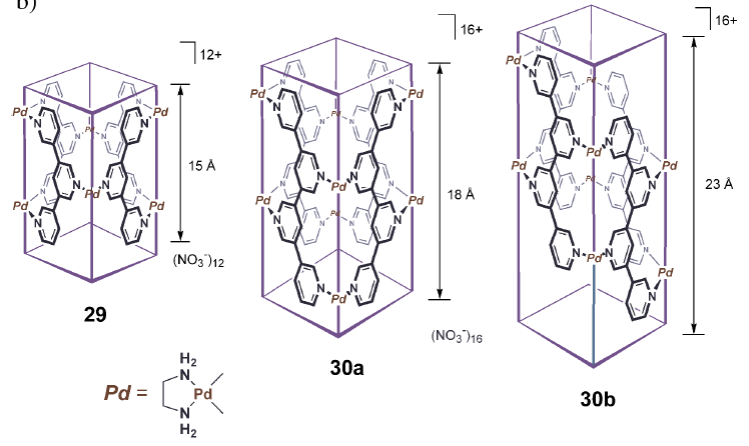


Effetto template

a)



b)



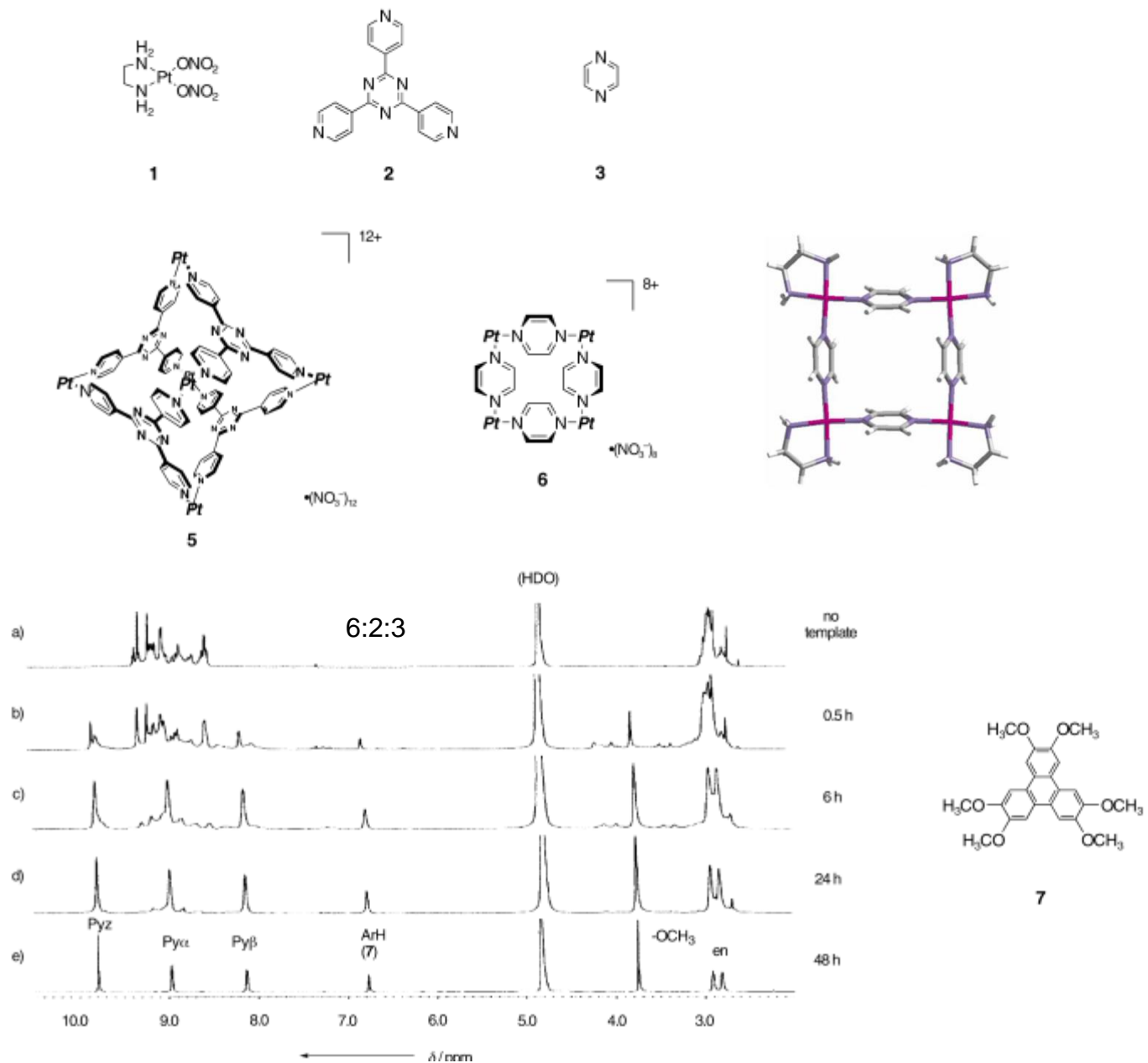
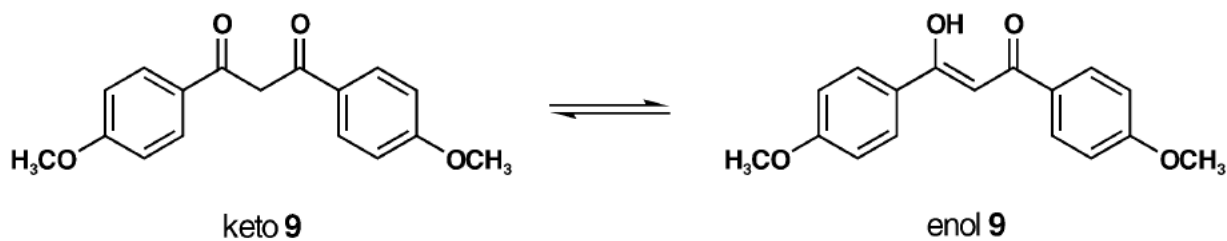
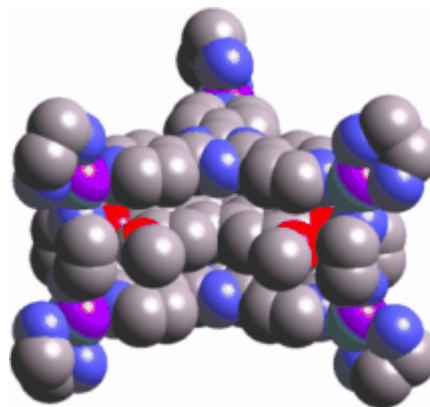
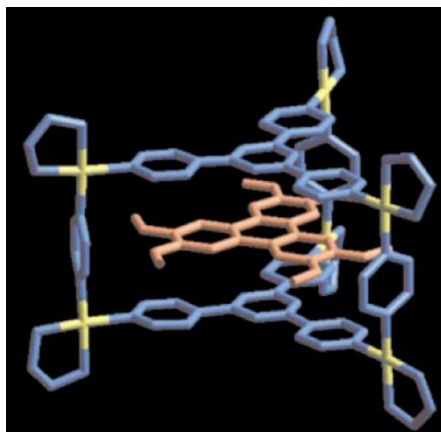


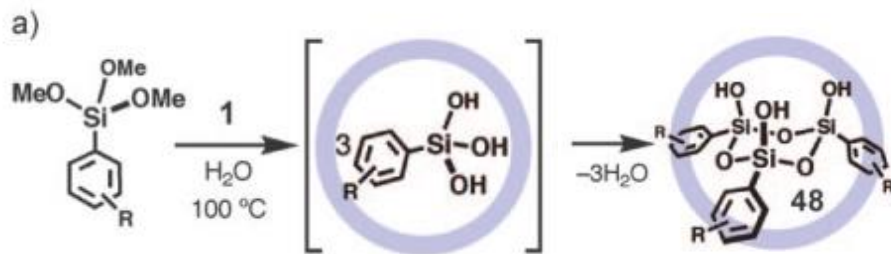
Figure 1. ¹H NMR spectra showing the guest-templated assembly of 7⊂4 complex (500 MHz, D_2O , 25 °C). a) A mixture of 1, 2, and 3. Template 7 was added to this solution and the mixture was heated at 100 °C for b) 0.5 h, c) 6 h, d) 24 h, and e) 48 h. Pyz = pyrazine.



The efficient intercalation of planar guest molecules within the cage was applied to the control of the equilibration between planer and nonplanar molecules. Keto and enol tautomers of β -diketone **9**, which exist in a 15:85 ratio in CD_3CN , can never be separated because of rapid tautomerization.

Stabilizzazione di intermedi reattivi: alcossi-silani ciclici

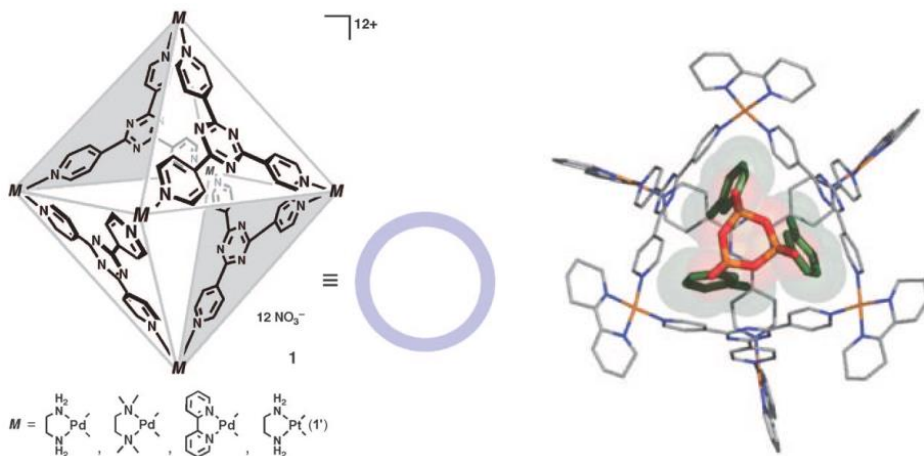
Ship in a Bottle



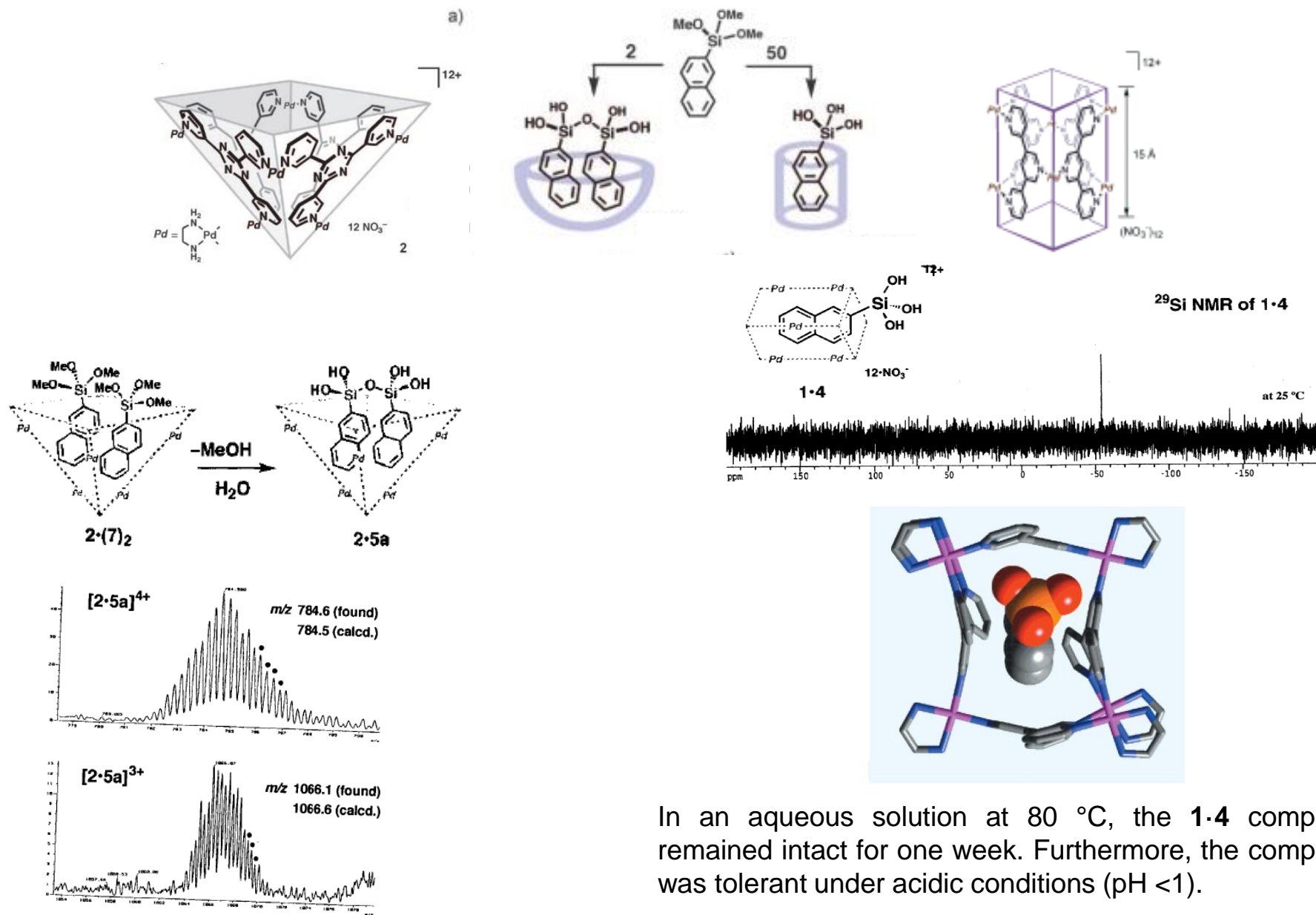
The roughly spherical cage cavity directs the selective formation of the cyclic trimer and prohibits further polycondensation despite the presence of labile Si-OH functional groups.

The stereochemistry of the condensation reaction is highly controlled within the cage giving only all-*cis* isomers.

The trimers prepared in situ can no longer escape from the cage because their dimension becomes larger than the portal size.



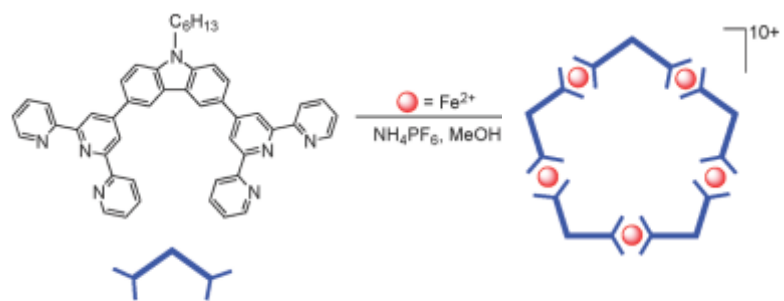
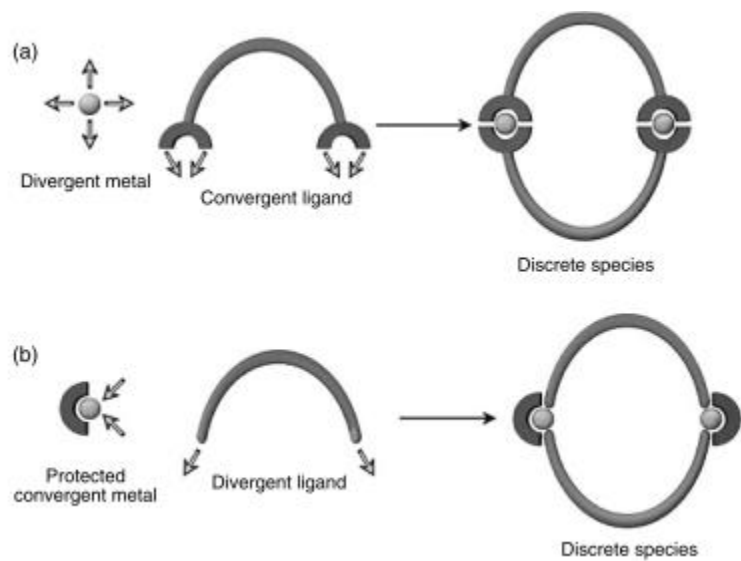
Stabilizzazione di intermedi reattivi: Oligomerizzazione di tri alcossi-silani

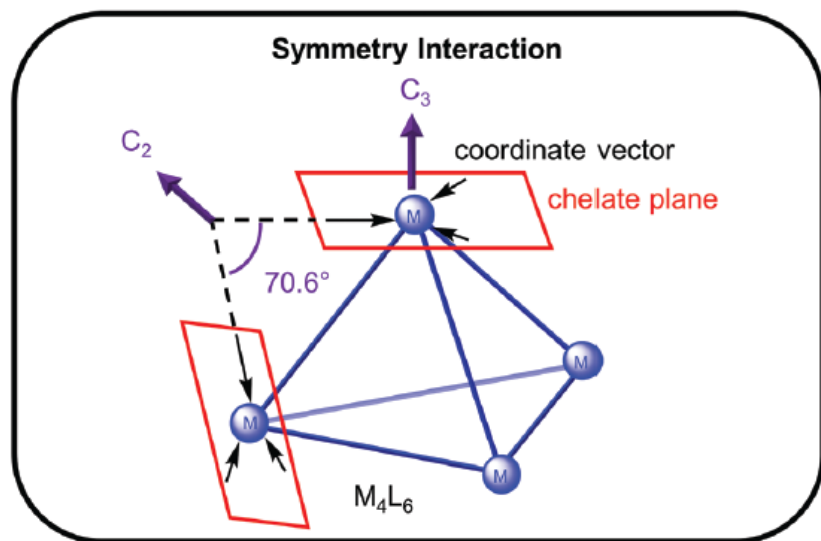


Diels-Alder in Aqueous Molecular Hosts: Unusual Regioselectivity and Efficient Catalysis

Michito Yoshizawa, Masazumi Tamura, Makoto Fujita*

Science 2006;312:251-254





Supramolecules by Design

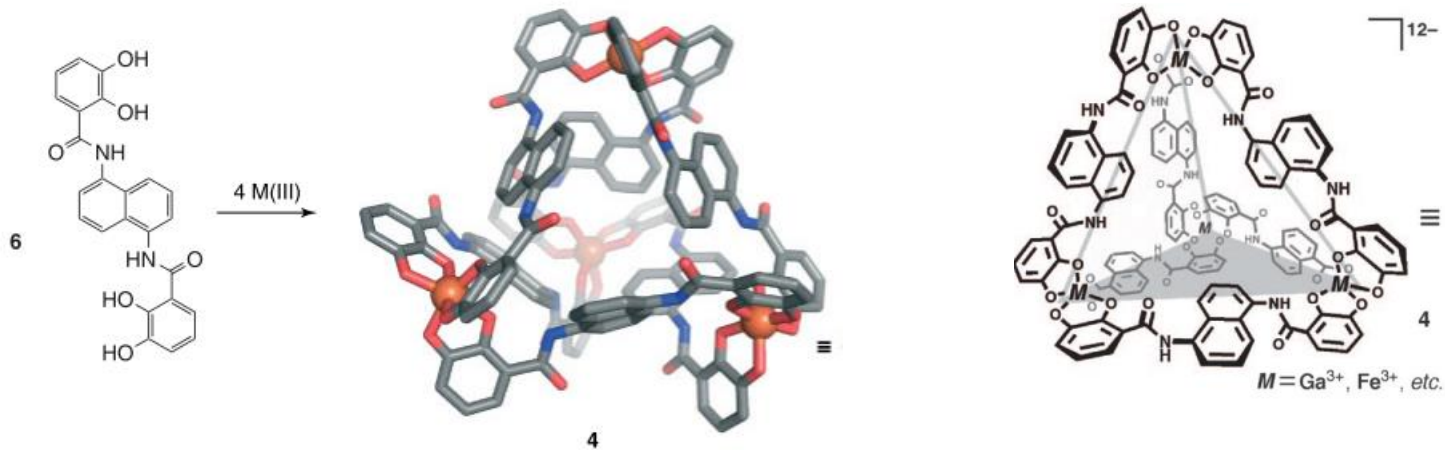
DANA L. CAULDER AND
KENNETH N. RAYMOND*

Acc. Chem. Res. **1999**, *32*, 975–982

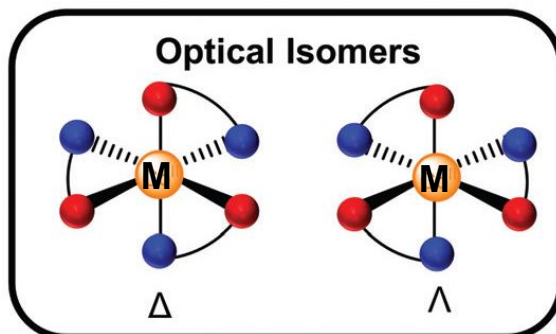
J. Am. Chem. Soc. **2001**, *123*, 8923–8938

Design, Formation and Properties of Tetrahedral M_4L_4 and M_4L_6
Supramolecular Clusters¹

Dana L. Caulder, Christian Brückner, Ryan E. Powers, Stefan König, Tatjana N. Parac,
Julie A. Leary, and Kenneth N. Raymond*



M_4L_6 , (Ga^{3+} , Fe^{3+} ; biscatechol-amidi) 12^- , $\Delta\Delta\Delta\Delta$, $\Lambda\Lambda\Lambda\Lambda$, 300-350 Å
 Stabilizzazione di cationi organici



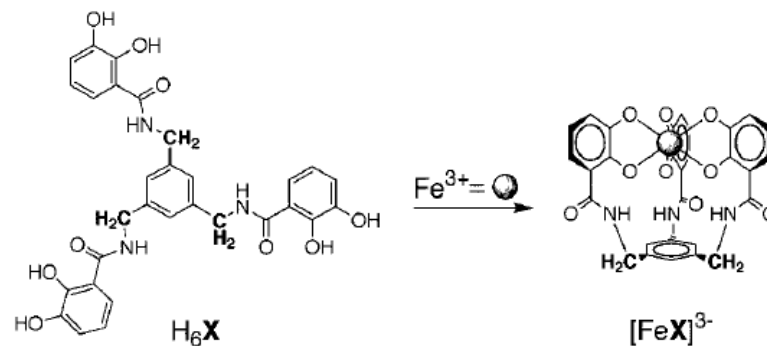
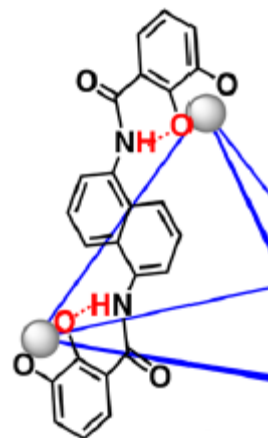
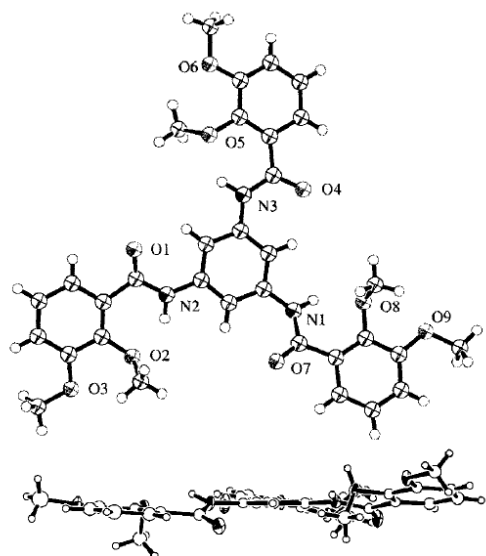


Figure 4. As shown in the enterobactin analogue H_6X , simple addition of a methylene group between the three-fold benzene scaffold and the catecholamide binding units gives the ligand enough flexibility to allow each of the arms to coordinate a single metal ion. This type of ligand flexibility must be avoided if multimetal clusters are desired.

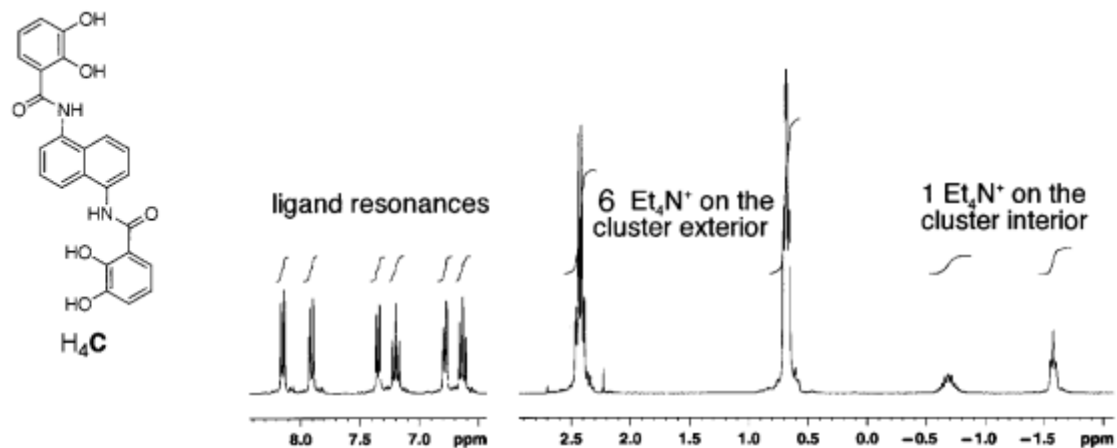


Figure 14. ^1H NMR (D_2O) depicting the two sets of Et_4N^+ resonances characteristic of the exterior and encapsulated cations.

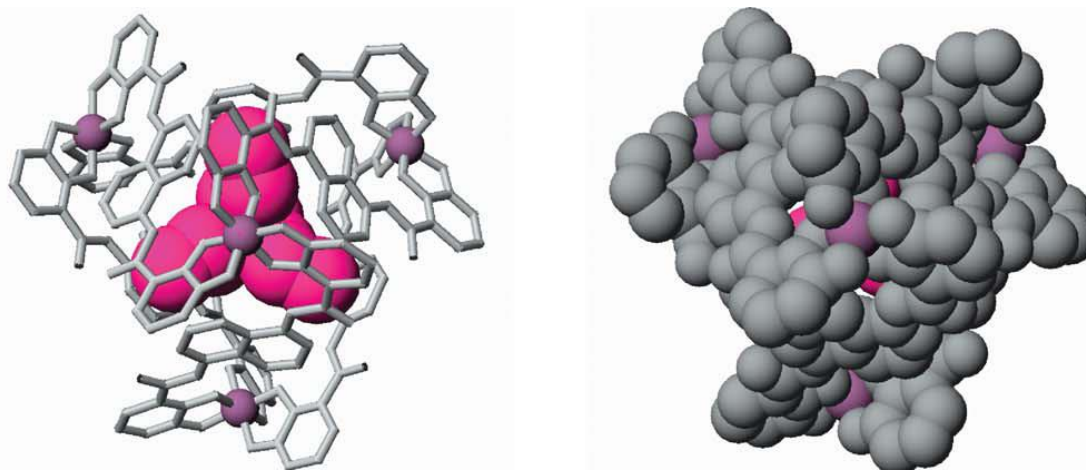
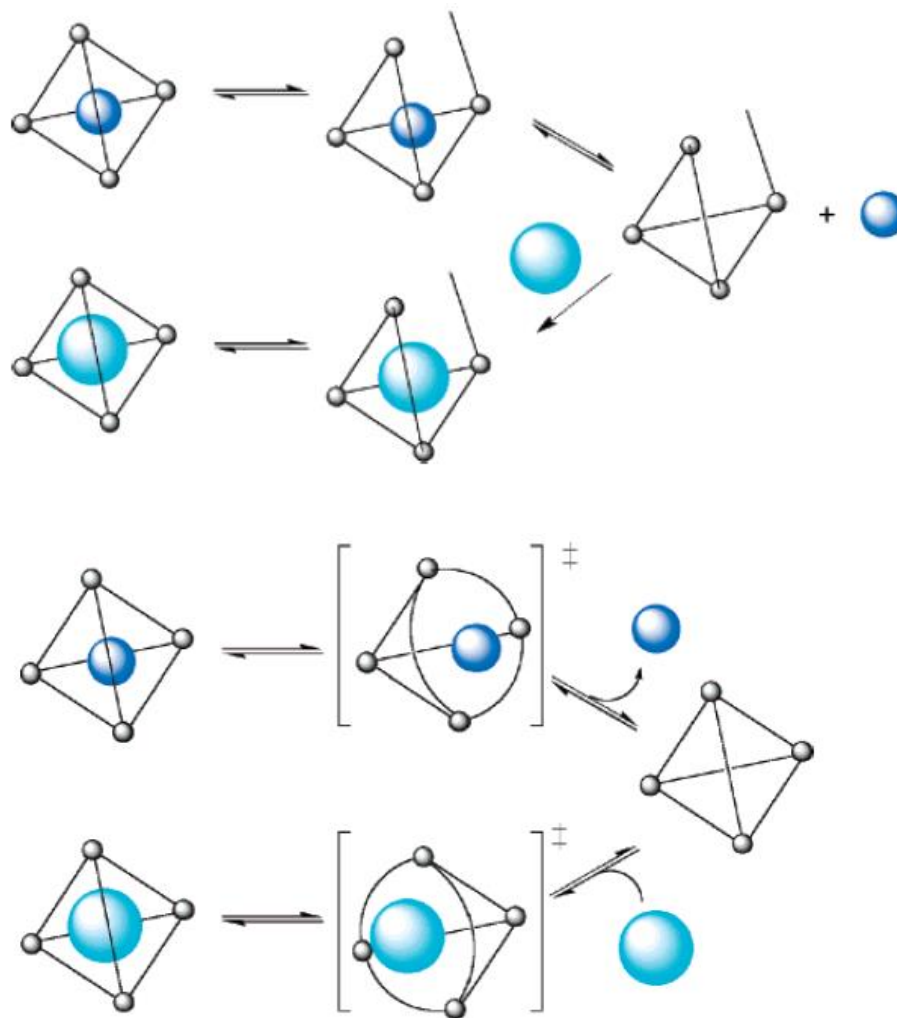
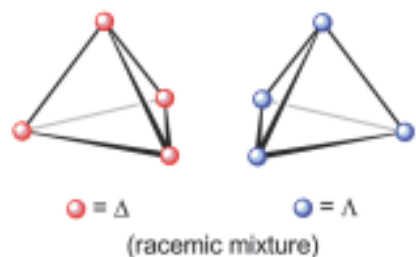


Figure 15. Based on the X-ray structure coordinates, $\text{Et}_4\text{N}^+[\text{Fe}_4\text{C}_6]^{12-}$ in both (a) wire-frame and (b) space-filling representations.

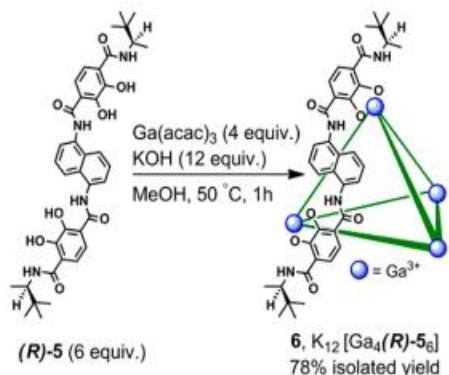
ESI-MS data

Guest exchange in an M_4L_6 supramolecular host has been evaluated to determine whether host rupture is required for guest ingress and egress. Two mechanistic models were evaluated: one requiring partial dissociation of the host structure to create a portal for guest passage and one necessitating deformation of the host structure to create a dilated aperture for guest passage without host rupture.





Resolution of the racemate using (-)-N'-methylnicotinium iodide: enantiopure $\Lambda\Lambda\Lambda\Lambda$ -(S-nic c cage) and $\Delta\Delta\Delta\Delta$ -(S-nic c cage) stereoisomers, after sequential ion exchange chromatography.



Achieving enantiopure M_4L_6 assembly without resolution using an amide-containing chiral directing group at the vertex of ligand - (R)-5 OR (S)-5.

6- $K_{12}Ga_4(R)-5_6$ and **6**- $K_{12}Ga_4(S)-5_6$ by CD spectroscopy: similar to those of $\Delta\Delta\Delta\Delta$ -cage and $\Lambda\Lambda\Lambda\Lambda$ -cage from racemate resolution.

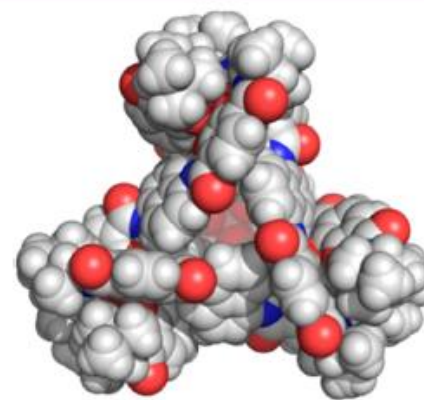
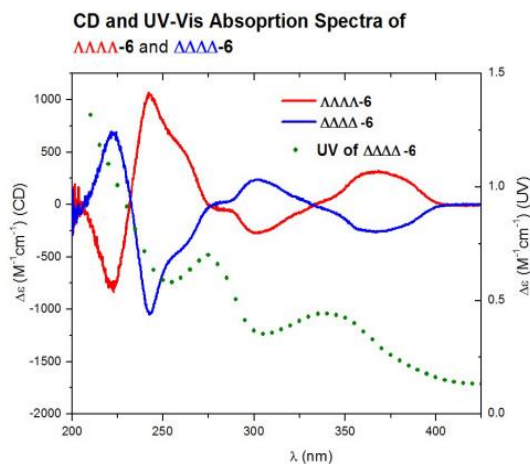
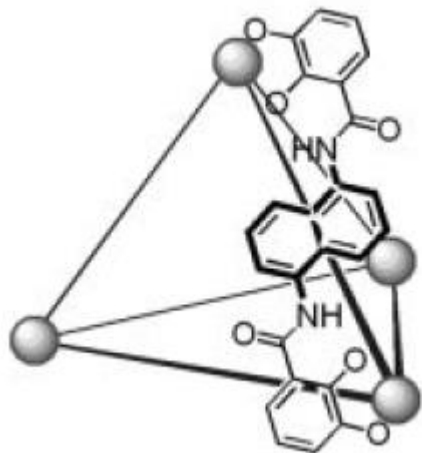


Figure 2. X-ray structure of $\Delta\Delta\Delta\Delta$ -**6**.



4

Addition of one equivalent of **4** to the $[\text{Ga}_4\text{L}_6]^{12-}$ assembly in D_2O results in the shift of the tropylium singlet from $\delta = 6.45$ to 2.95 ppm (Figure 4, a). Integration of this upfield-shifted tropylium signal indicates that this cation is encapsulated as a guest inside the tetrahedral assembly with a 1:1 ratio. Addition of a second equivalent of tropylium ion results in a second broad resonance at $\delta = 5.18$ ppm (Figure 4, b). The upfield shift of this resonance, compared to the resonance of free tropylium in D_2O , indicates that the second equivalent of aromatic tropylium cation interacts with the $[\text{Ga}_4\text{L}_6]^{12-}$ assembly by ion-pair association with the highly-charged assembly, as seen

After 20 h in solution (Figure 4, c), the encapsulated tropylium signal is still sharp, while the signal for the tropylium associated with the assembly was noticeably broadened, and the signal for free tropylium at $\delta = 6.45$ ppm is unobservable. Free tropylium completely decomposes in D_2O after approximately 24 h, so it seems that encapsulation of this cation in the hydrophobic environment of the $[\text{Ga}_4\text{L}_6]^{12-}$ cavity has significantly increased its stability.^[26]

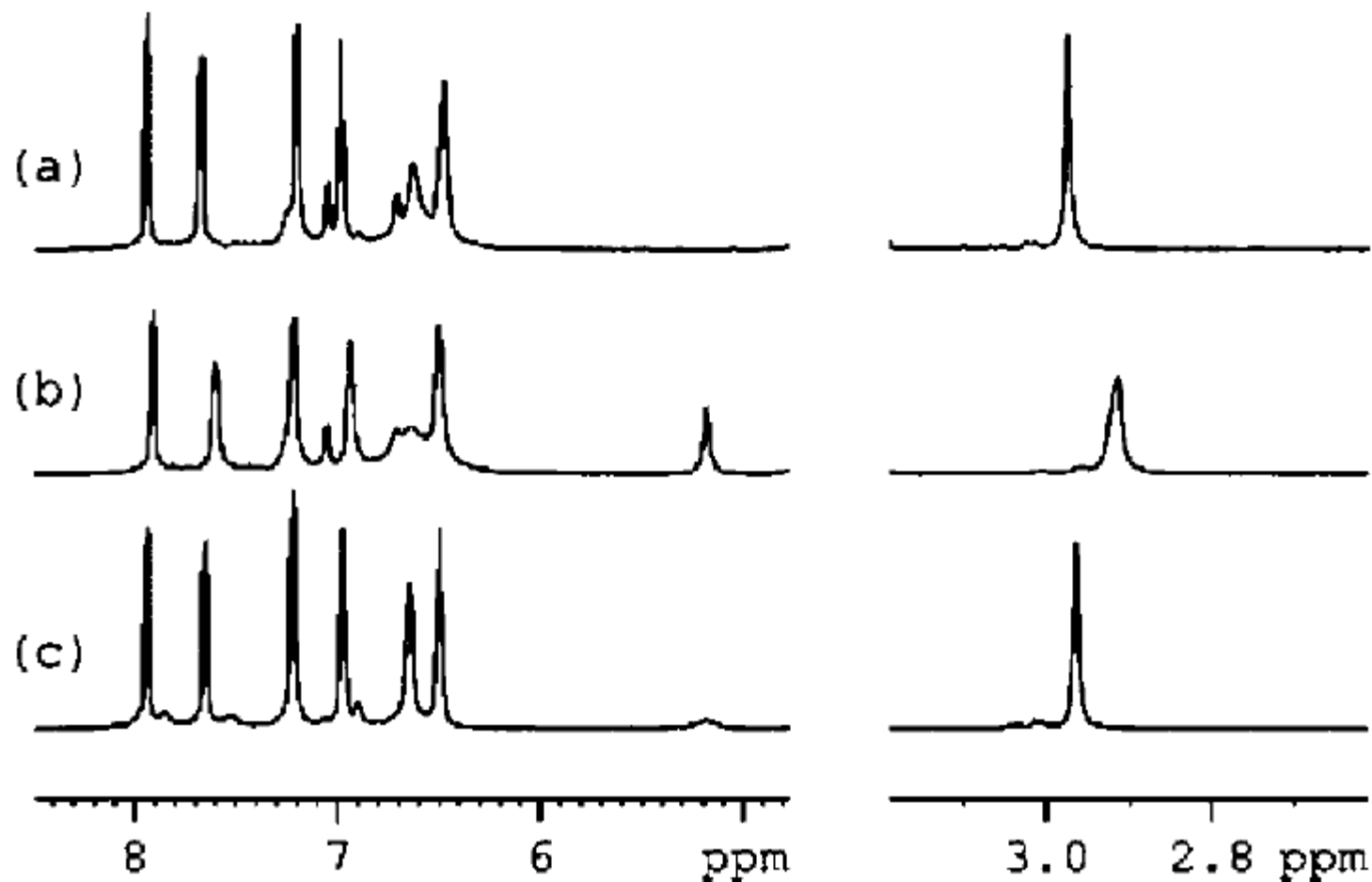
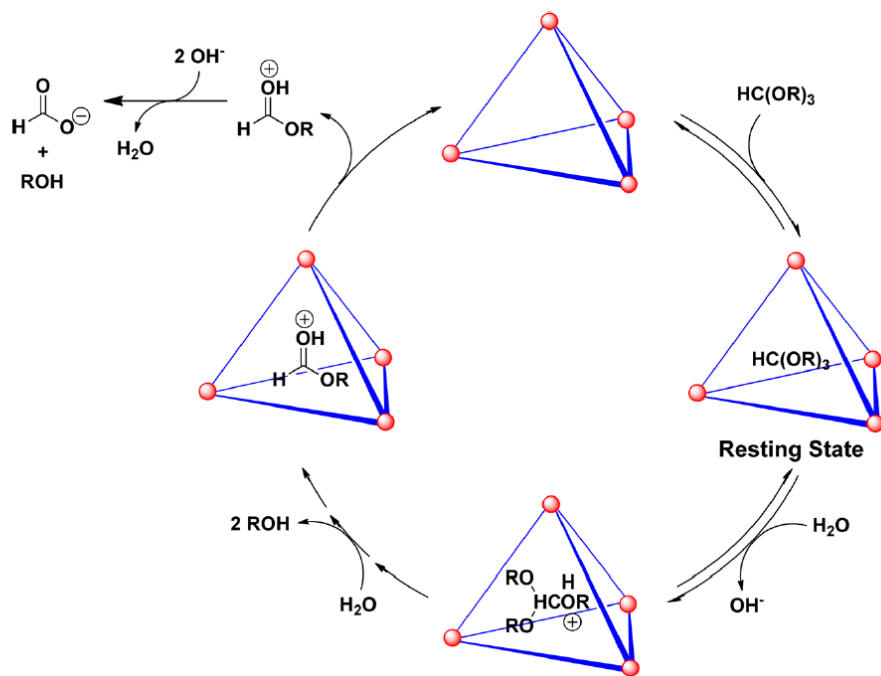


Figure 4. ^1H NMR spectra in D_2O of (a) the $[\text{Ga}_4\text{L}_6]^{12-}$ assembly + 1 equiv. **4**; (b) + 2 equiv. **4**; (c) sample in spectrum b after 20 h

Acid Catalysis in Basic Solution: A Supramolecular Host Promotes Orthoformate Hydrolysis

Michael D. Pluth, Robert G. Bergman,* Kenneth N. Raymond*

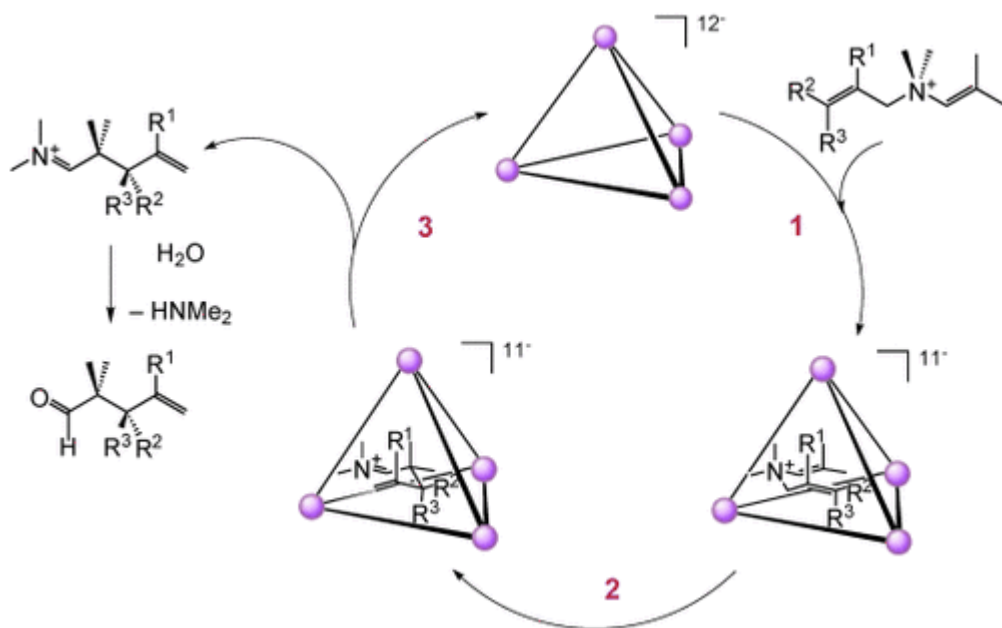


reached. Although the $\text{p}K_a$ of 3-H^+ is 10.8 in free solution, stabilization of the protonated form by **1**, which can be calculated as the product of the $\text{p}K_a$ and the binding constant of the protonated amine, shifts the effective basicity to 14.3 (32). This dramatic shift highlights the substantial stabilization of the protonated species over the neutral species upon encapsulation in the highly charged cavity (33).

Supramolecular Catalysis of a Unimolecular Transformation: Aza-Cope Rearrangement within a Self-Assembled Host**

Dorothea Fiedler, Robert G. Bergman, and Kenneth N. Raymond**

These findings highlight the ability of container-like molecules to provide size- and shape-defined nanospaces, highly capable of catalysis of unimolecular organic reactions. By binding the substrates in a reactive conformation, the host assembly accelerates the rates of rearrangement by up to



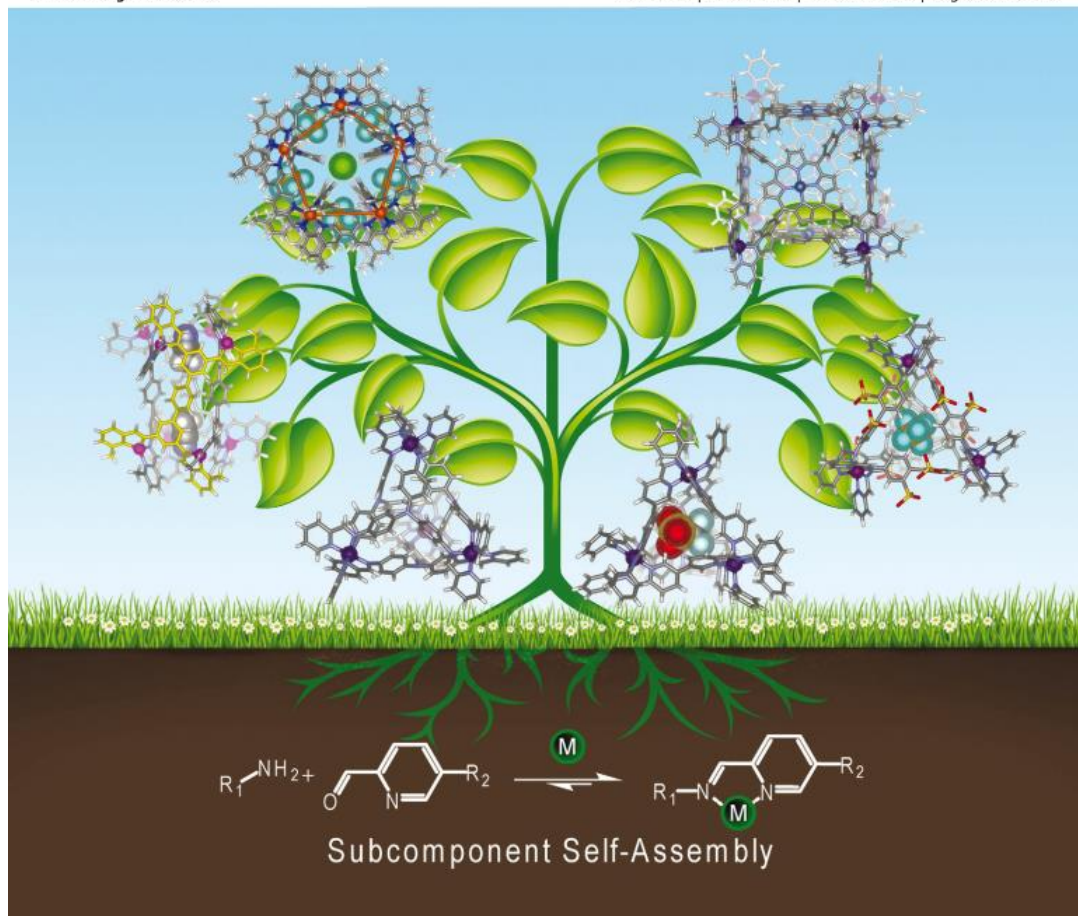
three orders of magnitude. Release and hydrolysis of the rearranged product generate catalytic turnover. With this, the large potential of supramolecular assemblies as synthetically useful tools in organic chemistry becomes apparent.

ChemComm

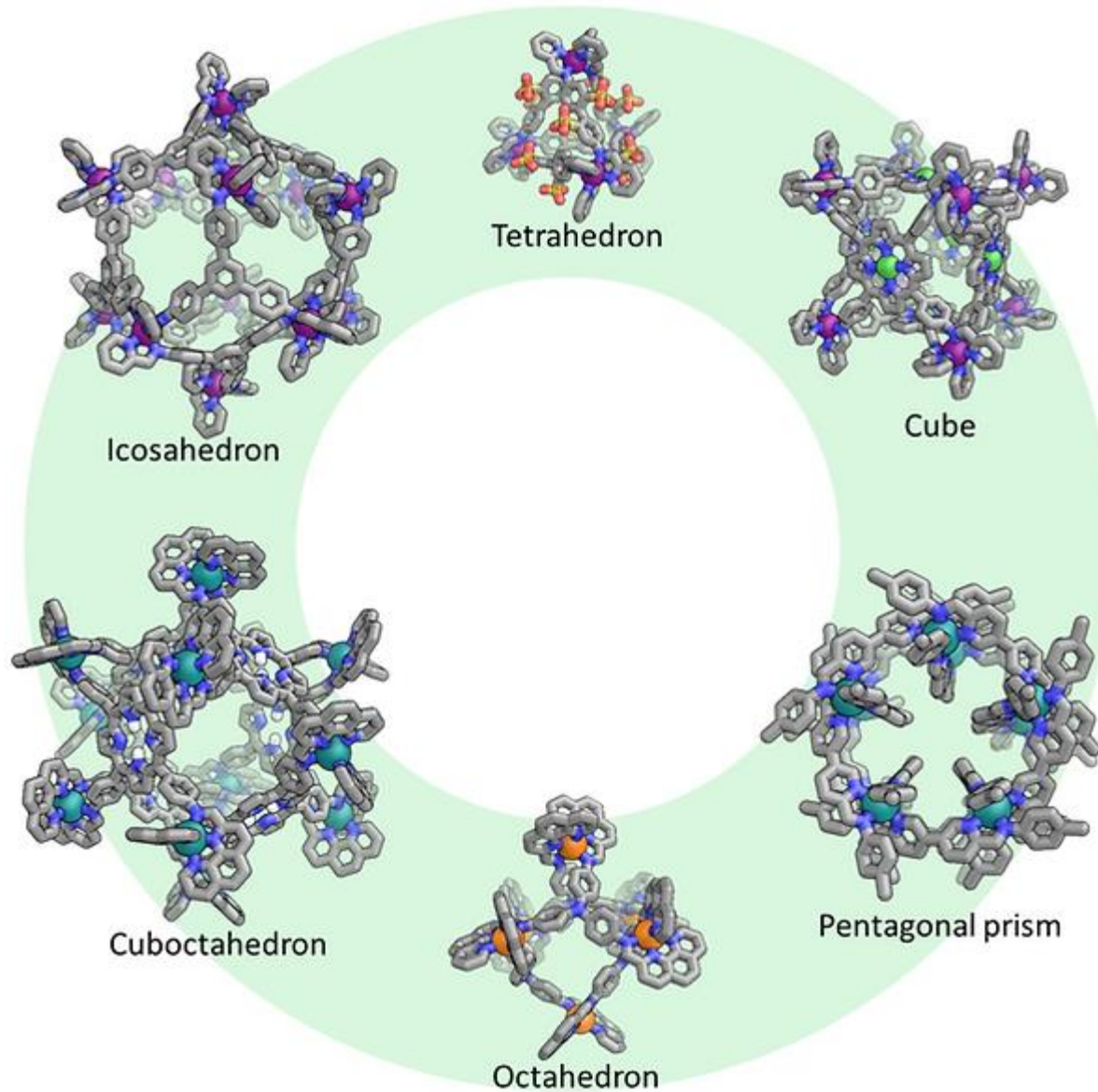
Chemical Communications

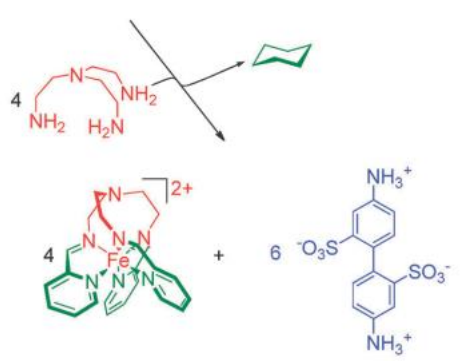
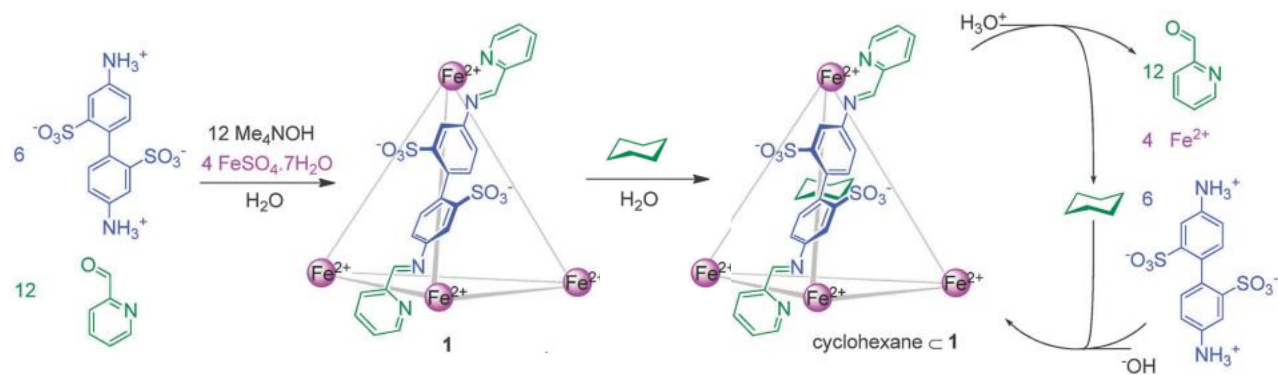
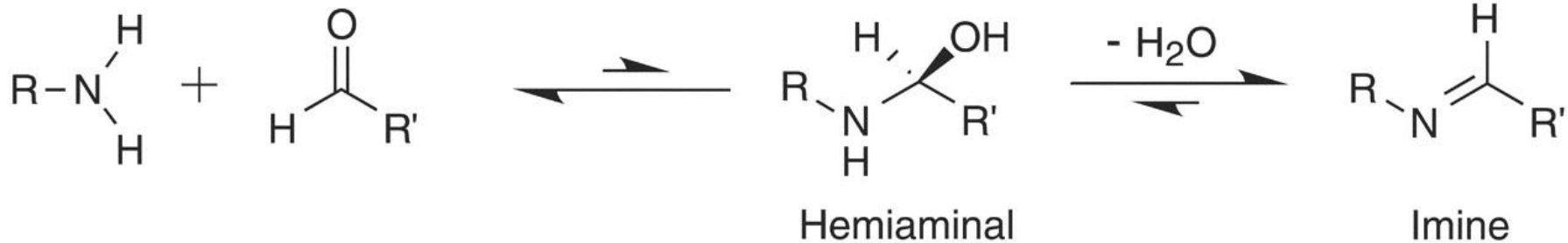
www.rsc.org/chemcomm

Volume 49 | Number 25 | 28 March 2013 | Pages 2465–2580

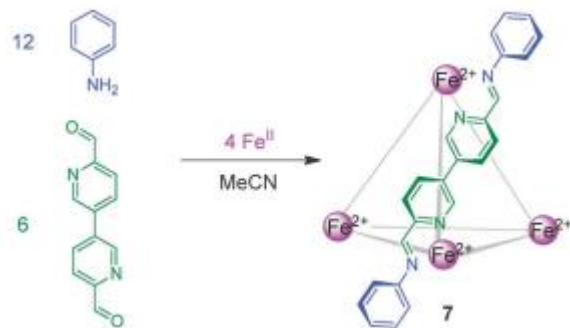
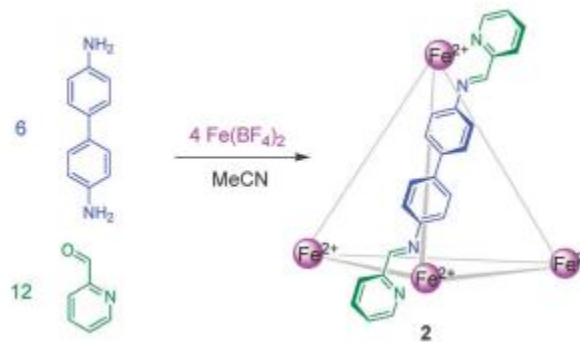


<https://www.nitschkegroup-cambridge.com/research-areas>

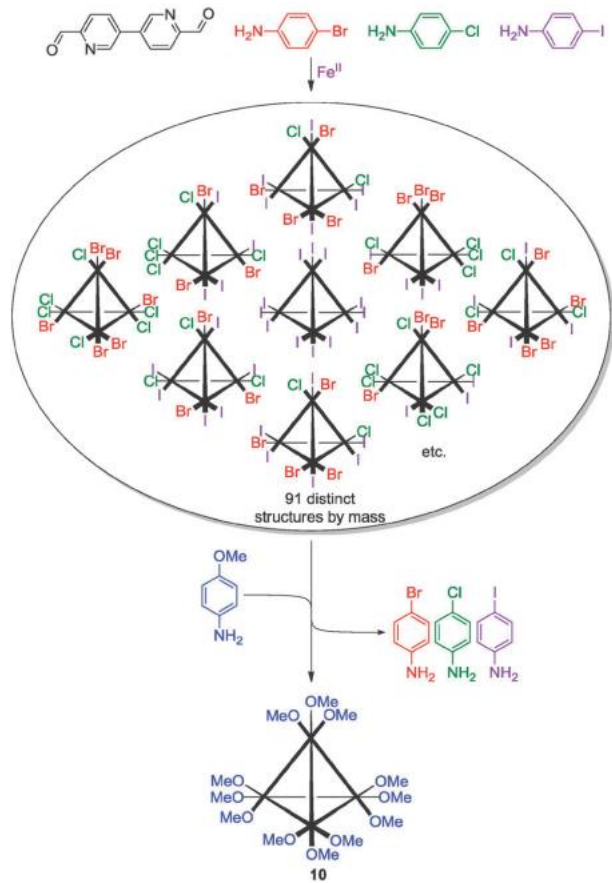
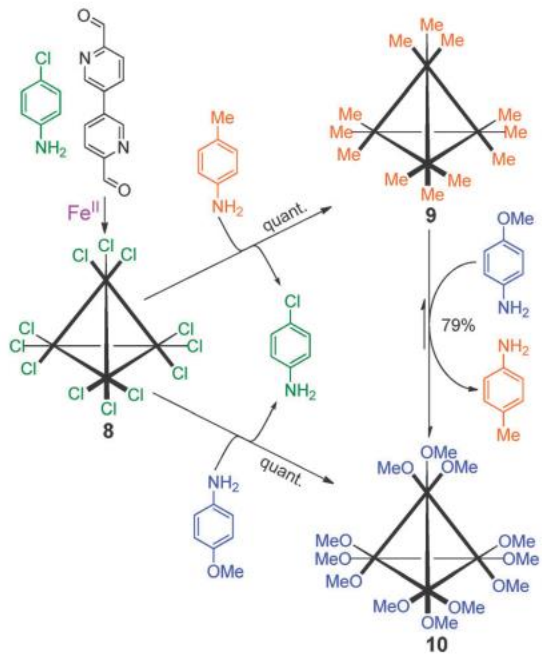


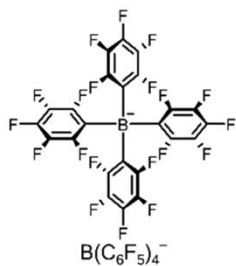
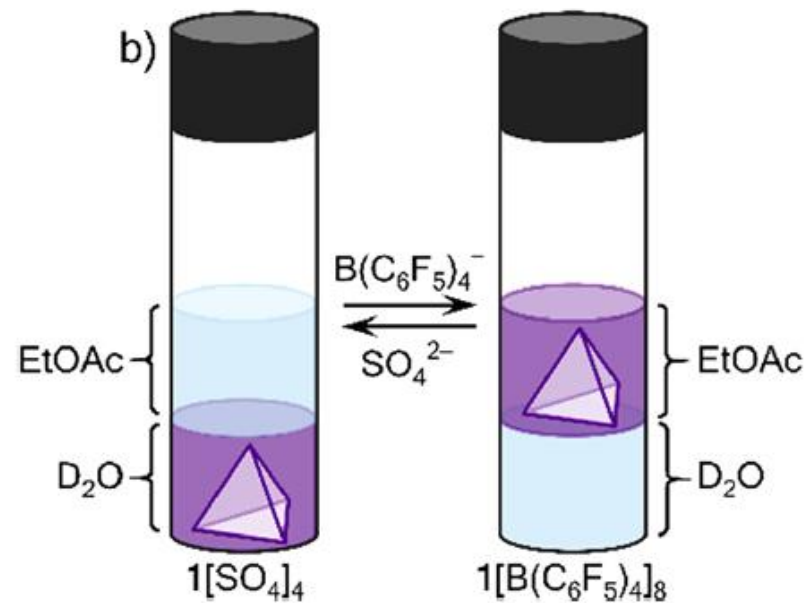
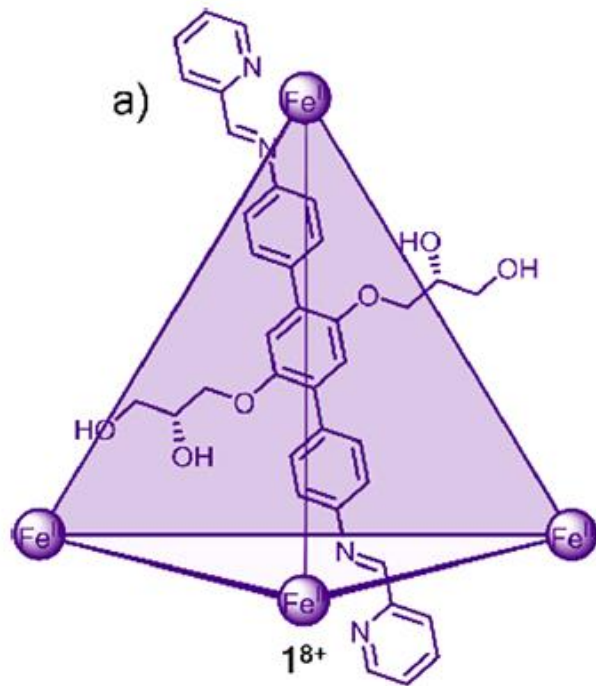


4,4'-diaminobiphenyl/2'-carbossaldehyde



6,6'-diformyl-3,3'-bipyridine/aniline





LiB(C₆F₅)₄ to promote anion metathesis from SO₄²⁻ to B(C₆F₅)₄⁴⁻

(*n*Bu₄N)₂SO₄ to regenerate the sulfate cage

White Phosphorus Is Air-Stable Within a Self-Assembled Tetrahedral Capsule

Prasenjit Mal,¹ Boris Breiner,¹ Kari Rissanen,² Jonathan R. Nitschke^{1*}

SCIENCE VOL 324 26 JUNE 2009

1697

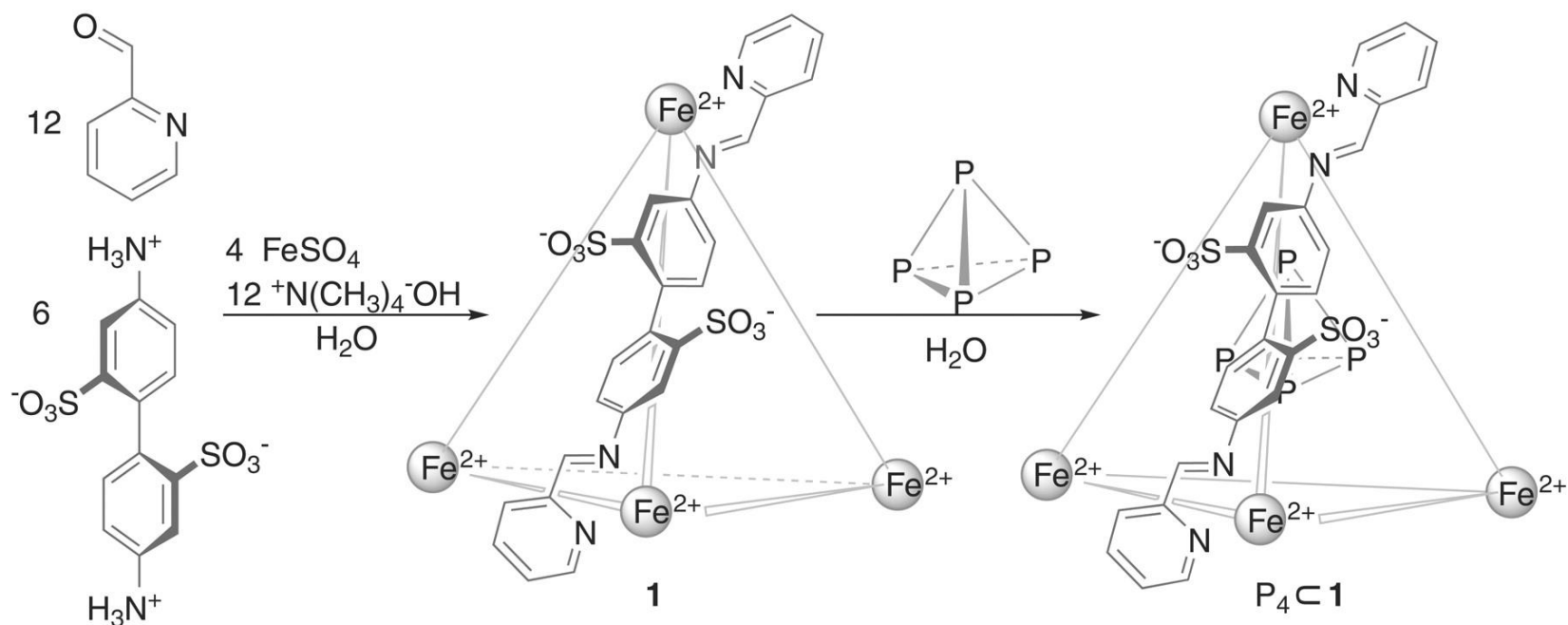


Fig. 1 Synthesis of tetrahedral cage 1 and subsequent incorporation of P₄.

Light-Powered Reversible Guest Release and Uptake from Zn_4L_4 Capsules

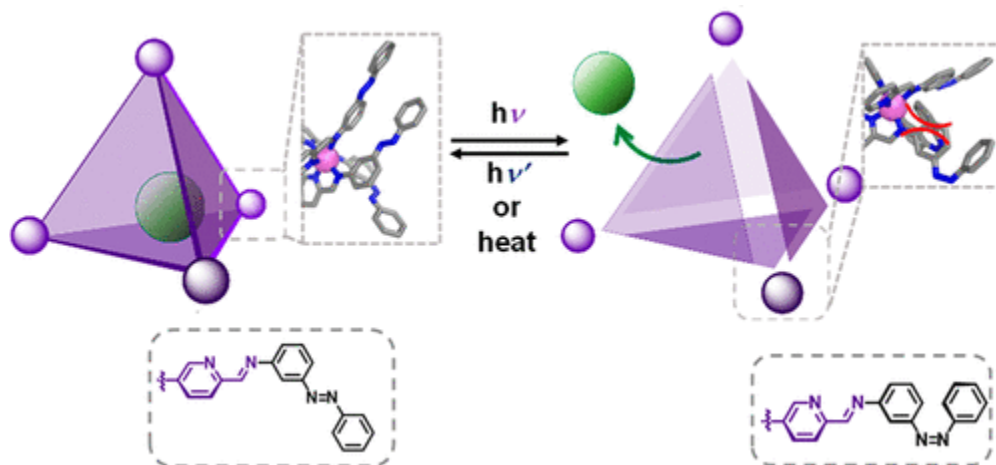
Amit Ghosh, Laura Slappendel, Bao-Nguyen T. Nguyen, Larissa K. S. von Krbek, Tanya K. Ronson, Ana M. Castilla, and Jonathan R. Nitschke*



Cite This: *J. Am. Chem. Soc.* 2023, 145, 3828–3832



Read Online



Choice of metal ion - coordination geometry + kinetic lability:

Octahedral - Ga^{III}, Al^{III}, Ti^{IV}, Fe^{II}, Co^{II}, Zn^{II}, Cd^{II}, Ni^{II};

Square planar - Pd^{II} and Pt^{II}

Lanthanide ions kinetically labile BUT variable coordination number and geometry

Kinetically inert metal ions (e.g. Ru^{II} and Ir^{III}): kinetic control unless *trans* effect.

The self-assembly process - interplay between enthalpy and entropy:

multiple equilibria/variety of factors - metal coordination geometry/kinetic lability/ligand geometry/metal-to-ligand stoichiometry/concentration/solvent/presence of guests.

Therefore, it can be difficult to predict the outcome since there is a delicate balance.

The principle of maximum site occupancy:

species where all the metal coordination sites are occupied with ligands are more stable than those with vacant coordination sites since this maximises the number of metal–ligand bonds and therefore, the enthalpy.

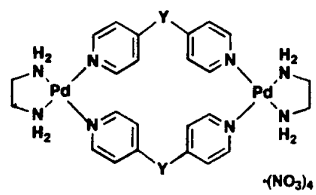
On the other hand, a system containing a larger number of smaller cages with fewer building blocks is favored on entropic grounds over one containing a smaller number of larger cages.

Multiple architectures can be self-assembled from the same building blocks:

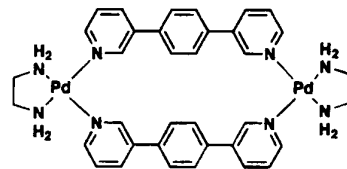
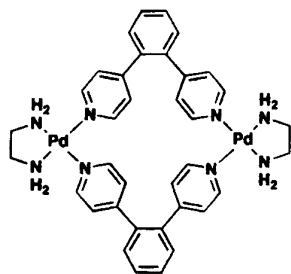
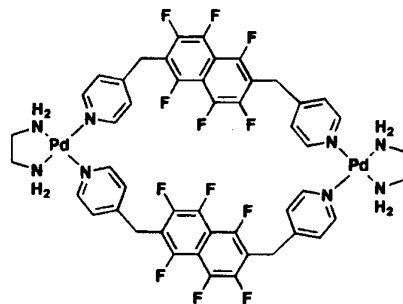
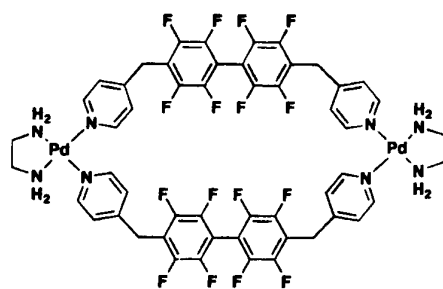
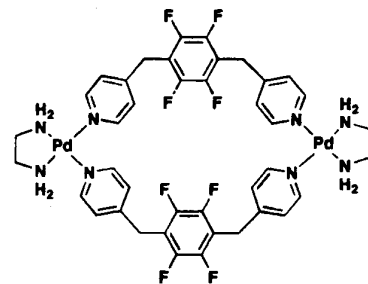
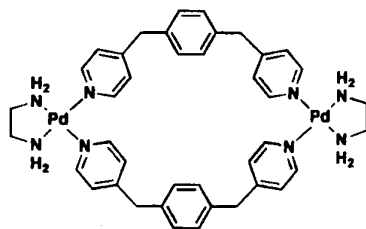
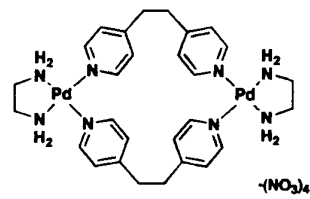
(a) a single cage when it is the thermodynamically most stable structure;

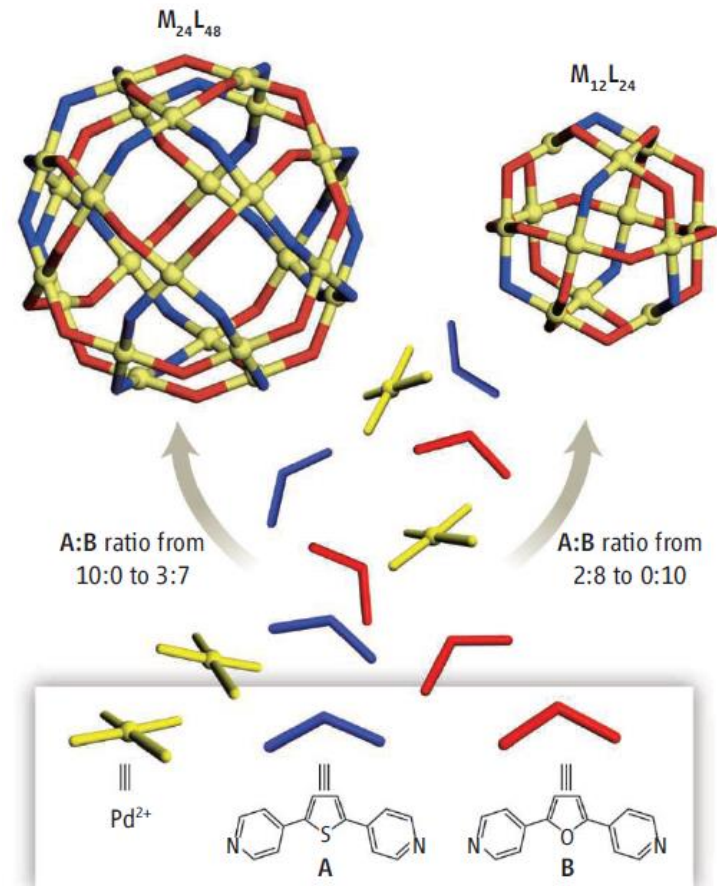
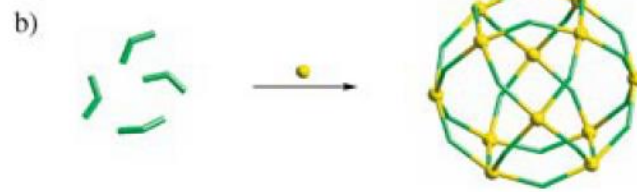
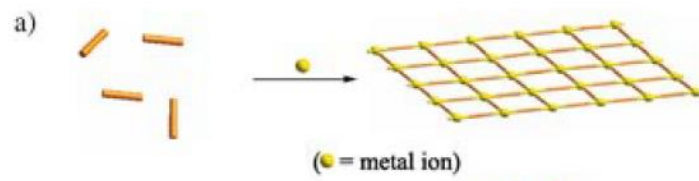
(b) a mixture of cages as the thermodynamic products with the distribution reflecting the relative energies of the cages;

(c) a dynamic combinatorial library with a large number of interconverting species in equilibrium.



Y = CH₂
Y = C(OH)₂





Design of lower symmetry cages

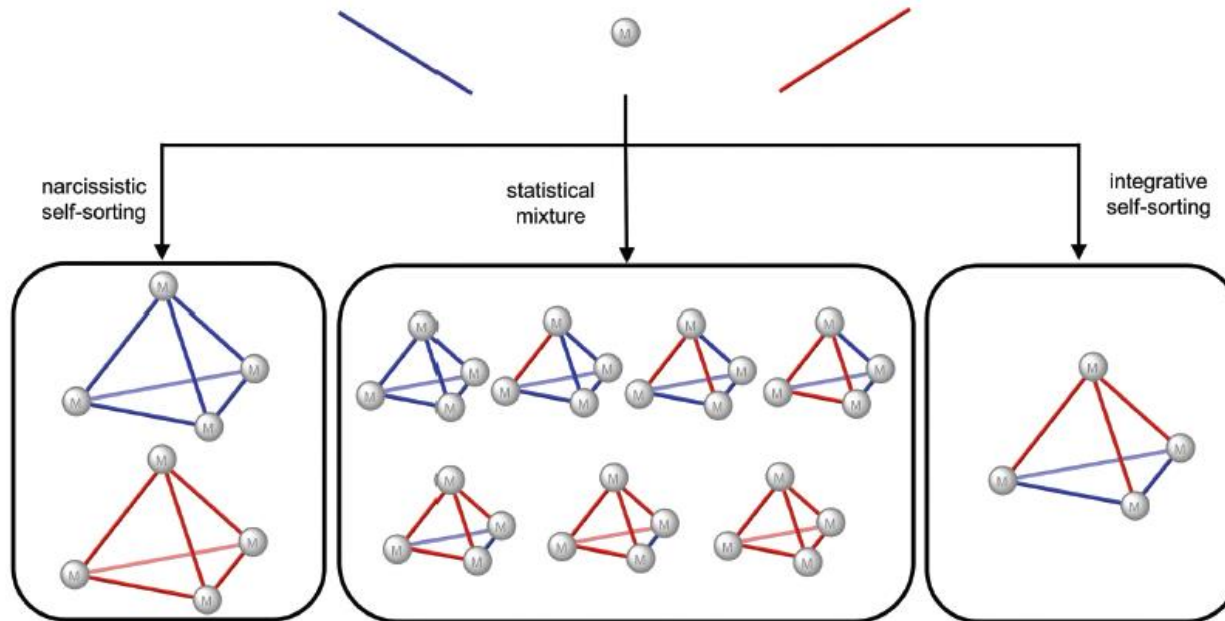
- symmetry breaking of the ligand upon metal coordination
- self-assembly of heteroleptic cages containing multiple ligands
- use of non-symmetric ligands to form homoleptic but lower symmetry cages
- use of multiple metals to form heterometallic cages.

Self-Sorting

narcissistic self-sorting - homoleptic cages with one ligand type in each cage

statistical mixture - both ligands are incorporated into the cages according to their statistical distribution;

integrative self-sorting - a nonstatistical distribution of heteroleptic cages results.



The key challenges to the design of heteroleptic cages via integrative self-assembly are, therefore, stabilisation of the heteroleptic cage/s relative to the homoleptic cages and biasing the system away from the statistical mixture.